

**EFFECTS OF INCLINED AND ECCENTRIC LOAD APPLICATION
ON THE BREAKOUT RESISTANCE
OF OBJECTS EMBEDDED IN THE SEA FLOOR**

CIRCULATING COPY
Sea Grant Depository

Prepared by
JOHN L. COLP and JOHN B. HERBICH
Coastal and Ocean Engineering Division
Texas A&M University

May 1972

TAMU-SG-72-204

COE Report No. 153

CIRCULATING COPY
Sea Grant Depository

EFFECTS OF INCLINED AND ECCENTRIC
LOAD APPLICATION ON THE BREAKOUT
RESISTANCE OF OBJECTS EMBEDDED IN
THE SEA FLOOR

by

JOHN L. COLP and JOHN B. HERBICH
Coastal and Ocean Engineering Division
Texas A&M University

Partially supported by the National Oceanic
and Atmospheric Administration Sea Grant Program
Department of Commerce Grant 2-35213

Sea Grant Publication No. TAMU-SG-72-204
Coastal and Ocean Engineering Division
Report No. 153 - C.O.E.

May 1972

ABSTRACT

The expansion of the field of coastal and ocean engineering has resulted in a great increase in applications for floating equipment anchored in shallow and deep water. Many of these applications impose a stringent station-keeping requirement. One of the solutions for such applications is the use of taut-line embedded mooring systems. Previous theoretical and experimental studies of such systems have been restricted to shallow-buried anchors with vertical load application. This study considers the forces required to break out model circular plate anchors embedded into three soil materials at depths of two and eight diameters when the load application is inclined from 90 degrees to 45 degrees from the horizontal and is attached from the mid-point over to one edge of the plate.

A review of past published contributions on the subject of mooring and anchoring systems, embedded anchors, and anchor withdrawal studies is included. Previous attempts at the explanation of the mechanisms invoked during anchor pullout using existing soil mechanics theory are discussed and the resulting quasi-theoretical equations are given.

A laboratory investigation of the displacements of individual particles of a simulated, dense, granular, cohesionless soil under inclined and eccentric load applications was conducted using a proven experimental technique involving a plane array of

cylindrical, steel rollers. The displacements of the particles were observed through a plexiglas tank face and were recorded photographically.

Model pullout tests using a three-inch diameter plate buried in tanks of three different soils - dense, dry, Ottawa sand; dense, submerged Ottawa sand; and Gulf of Mexico marine sediments - were performed. Maximum pullout forces required to breakout the model anchor under various inclined and eccentric load applications were recorded. The effects of two depths of burial - two plate diameters and eight plate diameters - were investigated.

Observations from the dense, dry sand tests indicated that the maximum required pullout force increased as the inclination angle moved from 90 degrees to 45 degrees from the horizontal. For the marine sediments investigated, the maximum pullout force also increased as the inclination angle changed but at a much smaller rate. The submerged sand deeply-buried pullout tests exhibited an anomaly in that the pullout force decreased at the 45 degree inclination. It is postulated that this result involves the action of pore water pressures activated during withdrawal.

The dense, dry sand tests indicated that, as the point of load application moved from the center to one edge, the maximum pullout force required decreased. The marine sediments exhibited a similar decrease but at a very slow rate for the deeply-buried case. The submerged sand deeply-buried tests displayed the same anomalous behavior as in the inclination study.

The data obtained from the dry sand and marine sediment model tests were examined using a dimensional analysis technique. A display of a dimensionless pullout force term containing inclination, eccentricity, plate diameter, and soil shear strength factors versus a dimensionless depth of burial term is given. Two distinct regions of the data, one for granular materials and the other for cohesive materials, were observed. A Wilson-Goodlet multiple regression analysis was performed and provided equations of a straight line for each material utilized in the experimental work which can be used for design purposes.

A bibliography containing fifty-three entries is included.

PREFACE

Research described in this report was conducted as part of the continuing research program in Coastal and Ocean Engineering at Texas A&M University.

The assistance of Don Murff, Ron Boggess and the staff at the Terramechanics Laboratory, Texas A&M Research Annex during the experimental portions of this study is gratefully acknowledged.

The suggestions and advice freely given by Dr. Charles H. Samson, head, Civil Engineering Department, Texas A&M University during the preparation of this report is truly appreciated.

The study was partially supported by the Department of Commerce Grant 2-35213 through the National Oceanic and Atmospheric Administration Sea Grant Program.

LIST OF CONTENTS

	Page
ABSTRACT	11
PREFACE	v
LIST OF CONTENTS	vi
LIST OF FIGURES	viii
INTRODUCTION	1
REVIEW OF LITERATURE	3
THEORETICAL CONSIDERATIONS	9
Dry Land Pullout Theories	10
Submarine Soil Pullout Theories	18
MODEL EXPERIMENT PLANS	22
EXPERIMENTAL APPARATUS AND PROCEDURES	25
Two-dimensional Tests	25
Three-dimensional Tests	29
EXPERIMENTAL RESULTS	34
DISCUSSION OF RESULTS	43
Two-dimensional Tests	43
Justification of Experimental Technique	43
Particle Displacements	45
Three-dimensional Tests	64
Soil Effects Considering Inclination	64
Soil Effects Considering Eccentricity	67
Dimensional Analysis	68

	Page
Dimensionless Design Relationship	72
CONCLUSIONS	80
Two-dimensional Investigation	80
Three-dimensional Investigation	80
RECOMMENDATIONS	83
BIBLIOGRAPHY	84
APPENDIX	89
Dimensional Analysis	89

LIST OF FIGURES

Figure		Page
1	Sketch of Pullout Test Apparatus	27
2	Anchor Plate	33
3	Definition Sketch	35
4	Photograph of Typical Two-dimensional Roller Displacements	37
5	Pullout Force Vs. Inclination, Roller Bearings and Dry Sand	38
6	Pullout Force Vs. Eccentricity, Roller Bearings and Dry Sand	39
7	Soil Effect on Pullout Force Vs. Inclination	41
8	Soil Effect on Pullout Force Vs. Eccentricity	42
9	Roller Pullout Test #1 - 90° , $d/b = 2$, $e/b = 1/2$	47
10	Roller Pullout Test #2 - $67\ 1/2^\circ$, $d/b = 2$, $e/b = 1/2$	49
11	Roller Pullout Test #3 - 45° , $d/b = 2$, $e/b = 1/2$	51
12	Roller Pullout Test #4 - 90° , $d/b = 8$, $e/b = 1/2$	52
13	Roller Pullout Test #5 - $67\ 1/2^\circ$, $d/b = 8$, $e/b = 1/2$	54
14	Roller Pullout Test #6, 45° , $d/b = 8$, $e/b = 1/2$	56
15	Roller Pullout Test #7 - 90° , $d/b = 2$, $e/b = 3/4$	58
16	Roller Pullout Test #8 - 90° , $d/b = 2$, $e/b = 1$	59
17	Roller Pullout Test #10 - 90° , $d/b = 8$, $e/b = 3/4$	61
18	Roller Pullout Test # 9 - 90° , $d/b = 8$, $e/b = 1$	62
19	Dimensionless Pullout Force Term Vs. Dimensionless Pullout Cable Inclination for Dry Sand	70

Figure		Page
20	Dimensionless Pullout Force Term Vs. Dimensionless Pullout Cable Eccentricity for Dry Sand	71
21	Dimensionless Pullout Force Term Vs. Dimensionless Pullout Cable Inclination for Marine Sediments	73
22	Dimensionless Pullout Force Vs. Dimensionless Pullout Cable Eccentricity for Marine Sediments	74
23	Dimensionless Pullout Force Term Vs. Dimensionless Inverse Eccentricity Term for Dry Sand and Marine Sediments	76
24	Dimensionless Pullout Force Term Vs. Dimensionless Burial Depth for Dry Sands and Marine Sediments	78

INTRODUCTION

The expansion of the field of coastal and ocean engineering has resulted in a great increase in applications for floating equipment anchored in shallow and deep water. Many of these applications also impose a stringent station-keeping requirement. One of the solutions for such applications is the use of taut-line mooring systems. However, these systems invoke a new and difficult problem in their design--that of loads on the anchor that are always more or less inclined from the vertical due to the current and wind action on the floating equipment. The effects of such load inclinations are not well known and, more basically, the phenomena of the resulting sea-floor soil failure caused by excessive inclined loads have not been observed and understood. As a result of these deficiencies of knowledge, the practicing ocean engineer is faced with the problem of including very conservative estimates of holding capacity in his anchor system design whenever inclined loads can possibly occur.

Closely related to the effects of load inclination on anchors is the problem of the effects of loads applied eccentrically to an embedded object. This problem is of concern to the marine engineer involved in the lifting of embedded objects (ships, submarines, etc.) from the sea floor during salvage operations. It

is known from experience that such operations must be made by applying the lifting forces eccentrically (near the ends of the embedded object). The sea floor soil failure phenomena invoked in such lifts and the optimum location of the eccentric lifting forces along the length of the embedded object have not been studied experimentally.

Reliable and economic designs of taut-line ocean bottom mooring systems require information on the effects of load inclination on the breakout resistance of embedded objects. An understanding of the sea floor soil failure phenomena and knowledge of the load factors required under such conditions are necessary.

Optimum results in terms of time and money in marine salvage operations involving the removal of objects embedded in the sea-floor require information on the effects of load eccentricity on the breakout resistance of such objects. Knowledge of the sea-floor soil failure mechanism during breakout and of the optimum location for load application would greatly facilitate such operations.

Figure 3 (p. 35) is a sketch defining the notation for the inclination of load application, the eccentricity of load application, the anchor plate diameter, and the pullout force used in this report.

REVIEW OF LITERATURE

The use of objects embedded in the sea floor (anchors) to moor ships since the Bronze Age (about 3500 B.C.) has been documented by Frost (18). Until quite recently, the selection of anchors for ships has been largely a trial and error process. The first evidence of organized research on the subject of anchor holding power (breakout resistance) appears to have been done by Howard and James (20) in about 1930. Since then, only a relatively few references (13, 14, 17, 25, 26, 29, 47, 49) on ship anchor research have appeared in the open literature.

Ocean engineering applications in the last decade or so have greatly increased interest in anchoring and mooring in deep-water (greater than 300 feet) locations. This increased interest has resulted in some studies of the general problem of breakout resistance of objects embedded in the ocean bottom. Most of this work is cited in bibliography entries 3, 4, 10, 11, 12, 16, 19, 21, 27, 28, 34, 35, 36, 41, 42, 43, 52. In approaching this problem, some of the researchers have used modern soil mechanics methods developed for dry-land applications of buried anchors to analyze breakout forces. Entries 1, 2, 15, 22, 30, 31, 32, 33, 40, 44, 51, cite some of the dry-land studies used. This approach may be a logical starting point for the ocean bottom work that has been done, since some portions of the ocean bottoms are composed of terrigenous sediments and might be expected to behave like submerged dry-land materials. On the other hand, most of the

deep-ocean bottom is covered by varying thicknesses of fine-grained, soft sediments. These sediments behave as non-Newtonian, viscous soil-water mixtures (soft muds and oozes). Breakout failure phenomena in such materials would not be expected to resemble those occurring in dry-land sediments which follow a Mohr-Coulomb type of failure mode. Because of the complications introduced when considering the actions of a viscous, non-Newtonian fluid; little, if any, work has been done on the breakout problem in this light.

The published literature on the problem of submarine soil breakout resistances can be divided into two types; (1) those of a general survey nature and (2) those that provide experimental and calculative results. Of the first type, Tudor (50) describes several mooring systems including the taut-line and states that the difficulty of designing a suitable mooring increases as the allowable amount of lateral excursion of the floating object decreases. He draws attention to the great extent of soft muds and oozes on the deep-ocean floor and to their viscous-like behavior in regard to breakout resistance. Another survey-type paper is that by Kéays (23). He comments on the lack of reliable design data on anchor breakout resistance available to an engineer, especially in the case of embedment anchors subject to vertical loads from taut-line moorings. Vesic (52) addressed the specific problem of breakout resistance of embedded objects in ocean sediments in a survey-like manner. He discusses the necessity of

considering (1) the effective weight of the object and soil mass, (2) shearing resistance of the over-burden soil, (3) effect of soil remolding, (4) effects of rate and character of loading, (5) soil adhesion force, and (6) soil suction force on the total breakout resistance. Vesic further notes that experimental work needs to be done on the effects of load inclination, load eccentricity, and soil liquidity.

The work of Balla (2) appears to be one of the earliest papers that treats breakout resistance using the experimental and calculative methods of modern soil mechanics. He experimentally determined the shape of slip surfaces resulting from the breakout of shallow-buried anchor plates in dense sand and presented a calculative method for pull-out force analysis based on his experimental observations. Mariupol'skii (30) performed experiments on determining breakout slip surface shape and calculated the state of stress in the soil above by assuming the mobilization of maximum shear stress in vertical cylindrical surfaces and that tensile failure occurs whenever vertical shear force exceeds soil shearing strength. Baker and Kondner (1) performed numerous small-scale pullout load capacity tests and developed empirical relationships using dimensional analysis. Their results confirmed Balla's results for shallow-buried anchors but revealed a distinction existing between shallow and deep-buried plates. Esquivel-Diaz (15) performed pullout tests on plates and piles in dense and loose sand, stiff silty clay, and very soft clay.

He verified the effect of burial depth and further related its effective location to soil type and condition. His experiments in clay demonstrated the effect of the soil suction force.

Full-scale field tests as well as large-scale laboratory experiments were reported by Muga (35). Based on his field tests, he proposed an empirical equation for calculating breakout force. Meyerhof and Adams (33) reported on results of two-dimensional and three-dimensional laboratory uplift tests in sands and clays. They presented an approximate general theory for uplift capacity of strip footings. They considered uplift capacity under vertical loads only and cited the need for research on the effect of inclined load application. Tolson (48) considered the vertical withdrawal resistance of small-scale cylindrical projectiles fired into laboratory soil bins. He developed an empirical equation to calculate the withdrawal resistance based on his observations. Smith (43) reports on several tests in which explosive embedment anchors were withdrawn from a variety of types of sea-floor materials. He did not attempt calculative efforts for data analysis.

Two very recent studies of breakout forces have been published. Both provide experimental and calculative results and are very valuable additions to the literature.

The report by Lee (27) describes the work done by the Naval Civil Engineering Laboratory in their study of breakout forces of objects embedded in cohesive soils over the past several years.

Data from field breakout tests in San Francisco Bay and the Gulf of Mexico; as well as from laboratory tests performed in 1968 and 1971 are given. This report is restricted to considering the problem of partially embedded objects only; that is, no data are presented in which the ratio of depth of burial to a significant dimension of the buried object is greater than one. Also, all of the embedded objects studied were three-dimensional (spheres, cylinders, or cubes) rather than plate-like items. Two modes of failure were considered. Immediate breakout where the pullout load was applied until failure occurred in a short time; and long-term breakout where a less-than-ultimate pullout load was applied and allowed to remain for a longer period of time until failure occurred. The analysis of the results provides procedures to be used in predicting forces required to remove partially embedded objects immediately and in estimating times required when lesser forces are required. The accuracy of the force prediction equation is shown to be about plus or minus 50% and the accuracy of the time estimate is about plus or minus 100%.

The report by Bembien, et al, (4) describes three years of work on determining the holding capacity of various types of marine embedment anchors as designed by the Naval Civil Engineering Laboratory. Both static and cyclic loads were applied during pullout. Tests were performed in sand, moist and saturated, and in saturated clay. Small-scale semi-spatial laboratory tests using a plexiglas-faced soil bin in which the soil materials were

layered with marker beds were performed to visually observe (and photograph) the marker bed deformations during pullout. These could be considered as three-dimensional tests sliced in half by the transparent face to allow visual access to the particle movements. The experimental data were used to develop empirical design curves for predicting anchor pullout resistance. Development of a theoretical solution to the problem of the prediction of the holding capacity of embedment anchors was not attempted. Investigation of the effect of other than vertical load application was not done.

THEORETICAL CONSIDERATIONS

The breakout of objects embedded in natural soil materials - whether it be a dry land soil or a sea-floor soil - is very definitely a problem of soil mechanics. Soil is an exceedingly complicated three-phase material thus making soil mechanics problems very complex. This complexity is perhaps best depicted in the introductory chapter of the recent book by Lambe and Whitman (24), who say:

Nearly all soil problems are statically indeterminate to a high degree. Even more important is the fact that natural soil deposits possess five complicating characteristics:

1. Soil does not possess a linear or unique stress-strain relationship.
2. Soil behavior depends on pressure, time and environment.
3. The soil at essentially every location is different.
4. In nearly all cases the mass of soil involved is underground and cannot be seen in its entirety but must be evaluated on the basis of small samples obtained from isolated locations.
5. Most soils are very sensitive to disturbance from sampling, and thus the behavior measured by a laboratory test may be unlike that of the in situ soil.

These factors combine to make nearly every soil problem unique and, for all practical purposes, impossible of an exact solution.

Application of the basic relationships of mechanics can provide a solution to a mathematical model of a soil problem. Indeed, this constitutes the so-called theoretical approach to soil

mechanics. Because of the assumptions that must be made to make the mathematical problem tractable, the nature and the variability of the soil material itself, and the unknown boundary conditions, the mathematical model being considered may not represent the actual soil problem. Thus the theoretical solution may not represent very closely a suitable solution to the soil problem. For these reasons much of the present-day engineering involving soils is based in major part on empiricism and engineering judgement - with whatever theoretical understanding that exists as a beneficial added ingredient.

Dry Land Pullout Theories

The few theoretical analyses of the pullout resistance of anchors buried in dry earth materials that have been attempted thus far have been forced to depend upon certain assumptions (more or less justified by experimental observations). That these assumptions are not justified for a general, all-inclusive case is evident from the discrepancies between calculated results and actual tests in soils. Although some investigators have been able to show rather good correlations between their theoretical calculations and observed test results under limited conditions, none of the theories have a universal applicability.

Balla (2) in the late 1950's developed a theoretical solution for determining the breakout load on a mushroom foundation. He noted that two methods of breakout load calculations had been used up until that time. One in which the shape of the breaking

out mass of earth was arbitrarily assumed and the weight of this earth was regarded as the breakout load required. The other in which the breaking out mass of earth was assumed to be a vertical cylinder with its cross section the same shape as the anchor plate and the breakout load was a combination of the weight of this earth mass and the shear resistance around its cylindrical surface. He disagreed with both of these methods and set out to determine the shape of the failure surface of the breaking out mass of earth using semi-spatial laboratory experiments. These experiments were performed in glass-faced tanks filled with air-dry sand having colored marker beds at intervals.

As a result of his tests, Balla concluded that it was clearly established that in all tests a single sliding surface developed and that it was a curve starting from the upper plane of the buried slab with a vertical tangent curving out from the axis in a circular shape and intersecting the free ground surface at an angle approximately equal to $(45^\circ - \phi/2)$.

Based on this conclusion, he proceeded to make a theoretical determination of the breakout load magnitude. He postulated that the breakout load consisted of two parts: the dead weight and the shearing resistance on the sliding surface. Assuming a plane stress state, cohesionless soil, and using Kotter's equation, Balla wrote the solution for the overall resistance against breaking out as:

$$F = d^3 \gamma [F_1 + F_3] \quad (1)$$

where F = total breakout force

d = depth of anchor

γ = unit weight of soil

$F_1 + F_3$ = coefficients which are functions of the
depth of burial in anchor diameters and
the angle of internal friction

In his paper, Balla plotted curves of the values of $[F_1 + F_3]$ for shallow-buried foundation slabs. Vesic (52) questions the accuracy of these values reported by Balla.

In the early 1960's, Mariupol'skii (30) approached the anchor plate breakout problem. He reasoned that the soil in the earth column above an anchor plate being subjected to a vertical pullout force was deformed by being compacted. As the soil above the plate became compressed the friction forces against the peripheral surface of the column increased since the vertical compressive stresses led to an increase of the radial stresses causing the friction forces. As the earth column moved upward, it subjected adjacent rings of earth to the effect of friction and cohesive forces, leading to the development of tensile stresses. He felt that tensile failure of the soil was the most probable mechanism by which an earth mass in the form of a cone with a curvilinear generatrix was separated from its original location.

Based on this reasoning, Mariupol'skii developed an equation for the total ultimate pullout force for a shallow buried anchor

plate of:

$$F = \frac{\pi}{4} (b^2 - b_0^2) \gamma d \frac{1 - (b_0/b) + 2K \tan \phi \, d/b + 4C \, d/b}{1 - (b_0/b)^2 - 2N \, d/b} \quad (2)$$

where. b_0 = diameter of anchor shaft

ϕ = angle of internal friction

K = coefficient of lateral earth pressure

N = empirical coefficient

C = cohesion of soil

Other terms were previously defined.

The empirical coefficient, K , was determined from laboratory experiments and was plotted by Mariupol'skii. Its value ranges from 0.0022ϕ to 0.0076ϕ where ϕ is in degrees.

Vesic (52) and others have pointed out that the assumptions made by Mariupol'skii in his initial reasoning on the failure mechanism of shallow anchors are entirely arbitrary and not in agreement with the elementary theory of earth pressure.

A solution for the pullout force of a deeply buried anchor was presented by Mariupol'skii in the same paper. Basing his approach on the assumption that the work done by the anchor during its upward movement should be equal to the work required to expand a vertical cylindrical cavity from the shaft diameter out to the plate diameter, he reached the following solution

for the ultimate pullout force:

$$F = \bar{W} + \pi b_o(d-b+b_o) f_o + \frac{\pi/4 (b^2 - b_o^2)}{1 - 0.5 \tan \emptyset} P_u \quad (3)$$

where: \bar{W} = effective weight of the anchor

f_o = unit skin resistance along anchor stem

P_u = ultimate pressure required for expansion
of a deep cylindrical cavity

The value of P_u was determined by Mariupol'skii by means of a trial and error solution.

Meyerhof and Adams (33) developed an approximate general theory of uplift resistance in soil for a shallow strip anchor defining "shallow" as a depth of burial at which the failure surface reaches the soil surface. They assumed a cylindrical failure surface extending along the length of the strip anchor. They modified their shallow strip solution for circular plate anchors and presented:

$$F = \pi cbd + s \left(\pi/2 \right) \gamma bd^2 K_u \tan \emptyset + W \quad (4)$$

where: c = unit cohesion

s = shape factor

K_u = nominal uplift coefficient of earth pressure
on vertical plane through footing edge

W = weight of soil above anchor

They plot values for K_u as a function of \emptyset and show it to be approximately 0.95 for \emptyset in the range of 30° to 45°. s is

shown as a function of d/b and ϕ , and is tabulated by Meyerhof and Adams.

For deep circular anchors (where h , the vertical distance above the footing to the top of the failure surface, is less than d) they show the ultimate pullout force as:

$$F = \pi c b h + s \left(\frac{\pi}{2} \right) \gamma b (2d-h) h K_u \tan \phi + W \quad (5)$$

Based on model tests, they observed that surface cracking as a failure mode occurred only when the anchors were at shallow depths. Reasoning that at great depths the flexing of the clay mass would be prevented by the overburden weight, they assumed that the pullout resistance would be determined by the shear strength of the clay. If this were the case, then the pullout resistance would be approximately equal to the bearing capacity of the clay. To analyze the results of their model tests, they used the following relationship which is analogous to the bearing capacity equation:

$$F = \left(\frac{\pi b^2}{4} \right) c N_u + \gamma d \quad (6)$$

where N_u = a dimensionless uplift coefficient

Experimental values of N_u were calculated from the observed pullout loads and plotted against d/b . They were observed to increase with depth to maximum values of 9 to 10.

Matsuo (31) studied the problem of the ultimate pullout resistance of an anchor consisting of a cylindrical shaft attached to a circular plate in an earth body assumed to be in a state of

ideal plastic equilibrium. He reasoned that, when a shear failure occurs in a soil mass due to the pullout force on a buried plate anchor, the earth pressure condition varies gradually from a semi-active condition in the vicinity of the plate to the passive condition at the ground surface. Hence the sliding surface was assumed to be a combined curve of a logarithmic spiral and its tangential straight line. The lower part being the spiral while the upper part is the straight line rising at an angle of $(\pi/4 - \phi/2)$ with the horizontal.

Working from this assumed failure surface, Matsuo expressed the ultimate pullout force as:

$$F = G + \gamma V + T \quad (7)$$

where: G = dead weight of footing

V = volume of soil mass within the sliding surface

T = vertical component of the resultant shearing resistance acting on the sliding surface.

Evaluation of Equation (7) resulted in the following expression:

$$F = G + \gamma(b_2^3 K_1 - V_3) + cb_2 K_2, \quad (8)$$

$$K_1 = \pi [(A-1)(A^2 F_1 + AF_2 + ABF_3 + BF_4 + F_5) + B],$$

$$K_2 = \pi [(A-1)(AF_6 + F_7) + B(B \tan \alpha + 2)]$$

where b_2 = horizontal distance from the shaft centerline to the point where the log spiral meets the straight line.

$A, B =$ coefficients of sliding surfaces
 $c =$ unit cohesion of soil
 $V_3 =$ volume of shaft below surface
 $\alpha = \pi/4 + \phi/2$

Matsuo gives the equations necessary to calculate F_1 through F_7 and also plots them in his paper.

For cohesive soils, Matsuo modified the equation above to give:

$$F = G + \alpha (b_2^3 K_1 - V_3) + cb_2 K_2,$$

$$K_1 = \pi [(A-1)(A^2 F_L + AF_2 + ABF_3 + BF_4 + F_5) + B], \quad (9)$$

$$K_2 = \pi [(A-1)(AF_6 + F_7)]$$

Matsuo performed many laboratory pullout tests in sands and loam using several different anchor plate shapes. His experimental data correlated very well with his calculated results.

In a later paper, Matsuo (32) derived an approximate calculation method for Equations (8) and (9) and compared his calculated results with the experimental results of others and with some of his field tests.

In the early 1960's Vesic (51) studied the effects of detonating an explosive charge in earth materials. As a result of this study he has proposed a theory giving the ultimate pressure

within a cavity in a homogeneous, isotropic solid. He assumes that the solid surrounding the cavity is rigid plastic to a certain limit, while beyond this limit it becomes linearly deformable.

The ultimate cavity pressure can be determined from a vertical equilibrium equation of the ruptured mass above the cavity. It is given by Vesic (52) in the form:

$$q_o = cF_c + \gamma dF_q \quad (10)$$

where. F_c and F_q = cavity expansion factors

He modifies Equation (10) for embedded plates and presents it as:

$$q_o = c\bar{F}_c + \gamma d\bar{F}_q \quad (11)$$

where: \bar{F}_c and \bar{F}_q = plate breakout factors.

The values for these factors are tabulated in his paper (52) for various values of ϕ and d/b .

Submarine Soil Pullout Theories

The Naval Civil Engineering Laboratory has performed or sponsored most of the research work done on pullout forces of objects embedded in submarine soils (4, 27, 28, 34, 36, 42, 52). The Navy's initial interest in the magnitude of pullout forces from ocean bottom materials stemmed from requirements for salvage operations or for deep submergence vehicle use. Accordingly,

their early studies were concerned only with partially embedded objects; i.e., those in which d/b was one or less. More recently, the work by Bembem et al (4) has looked at the pullout of deeply placed embedment anchors.

In all cases, the Navy work has emphasized the development of empirical equations for determining pullout force that would be available for immediate use. Little has been published in their reports on the development of a theoretical model of pull-out forces in submarine soils.

Lee (27) does describe the formulation of a breakout equation based on the theoretical bearing capacity equations as developed by Prandtl and by Skempton. He presents a breakout force equation as:

$$F = 5 SA \left(1.0 + 0.2 \frac{d}{b}\right) \left(1.0 + 0.2 \frac{b}{L}\right) \quad (12)$$

where: F = breakout force carried by soil
 S = undrained shear strength of soil
 A = object cross-sectional area
 d = embedment depth
 b = smallest lateral object dimension
 L = object length

Lee compares the results of many NCEL shallow embedment tests, both in the laboratory and in the field, to the calculated results of the above equation and shows rather poor correlation. He then proceeds to develop an empirical relationship to his test data.

In summary, it can be said that the state of the art in theoretical considerations of pullout forces of buried objects, either in dry land or in the submarine environment, is rather poorly developed. Those theoretical approaches that have been taken agree with observed physical results only in rather limited cases and none of them appears to have a general application to the overall problem.

It appears that the inability of pullout theories to perform universally lies with the difficulty of predicting the proper failure surface in the multiplicity of soil environments. In bearing capacity theory, the stresses are distributed below the footing in a continuous medium which can be assumed to be homogeneous and isotropic. Therefore, the geometry of the failure zone is predictable. In pullout theory, the stresses are distributed above the anchor plate and their distribution is uniquely influenced by the surface boundary and its location.

In many submarine soils, the problem of pullout theory is even more complex because of the non-Newtonian characteristics of the sea-floor sediments. A possible approach to a useful theory under this environment might be to use suitable rheological relationships considering some viscosity-type failure criterion, rather than those used for the various dry land solutions.

Finally, the pullout of buried objects in soil is a non-conservative mechanics problem. Thompson (46) says: "The fact is present day mechanics are inadequate for the solution for non-conservative mechanics problems for even the simplest of materials such as air or water".

MODEL EXPERIMENT PLANS

The initial laboratory tests were designed to allow the visual observation, in a two-dimensional array, of particle motion of a simulated, dense, cohesionless, granular material during pullout of a plate under the application of inclined and eccentric loads. This particle motion information would assist in the planning of further needed tests in a three-dimensional array. Any problems as to load inclination and eccentricity that might arise could be seen visually and corrected before proceeding into the more time-consuming, three-dimensional test series. Also, the failure phenomena that occurred during these modes of loading could be observed which would aid in understanding them.

The data taken during this series consisted of the value of the maximum pullout load and a sequence of 35-mm photographs showing the motion of the individual particles at discrete intervals during the pullout.

The second series of planned tests was performed in a three-dimensional tank of dense, air-dry Ottawa sand. This material was selected because:

1. Being a uniform, cohesionless, granular material, it was a direct three-dimensional analog of the two-dimensional tests performed in the first series. The particle motions visually observed in the first series could be expected to be duplicated in three-dimensions in this material.

2. It is a standard material commonly used in soil mechanics research whose actions under loading have been observed by many researchers.
3. The personnel at the Texas A&M Terramechanics Laboratory, where these experiments were performed, have used this material extensively in past penetration experiments and have perfected methods for constructing uniform, homogeneous test samples that have been demonstrated to have repeatable properties as reported by Murff and Coyle (37, 38).

The data taken during this series consisted of maximum pullout load for each of the conditions of load inclination, load eccentricity, and depth of burial.

The third series of tests was performed exactly as was the second series except that the dense, Ottawa sand samples were submerged under fresh water. Submergence was accomplished in the manner previously used at the Terramechanics Laboratory and described by Murff and Coyle (38). This series of tests was expected to be analogous to those in the second series, but would show the effects of submergence. The same data were taken as in the previous series.

The fourth and final series of tests was that performed in the same manner and on the same equipment as were series two and three except that the soil sample was actual sea-floor sediments obtained from the Gulf of Mexico by the Texas A&M Geological Oceanography Division. The selection of this material was made to compare the differences in pullout force and failure mechanisms that occur between a fine-grained, marine material

and the granular materials examined in the second and third series.

EXPERIMENTAL APPARATUS AND PROCEDURES

All of the experiments conducted for this study were performed at the Terramechanics Laboratory at the Texas A&M Research Annex. This laboratory was developed jointly by Texas A&M University and Sandia Laboratories for the purpose of earth penetration research.

Two-dimensional Tests

The two-dimensional tests were conducted in a tank measuring three feet high by four feet wide by three-fourths of an inch thick. The three-foot by four-foot faces were made of plexiglas. The tank contained an array of approximately 150,000 steel rollers from commercial needle bearings. The rollers were cylinders about one-eighth inch in diameter and three-fourths inch in length. They were arranged such that all of the cylindrical axes were parallel, with the ends facing the plexiglas faces of the tank. The ends of the rollers were large enough so that in photographs of the array taken through the plexiglas, each roller is visible and its displacements can be observed. This equipment has been used extensively in the past for penetration studies and it is described and shown in photographs by Colp (9) and Thompson (45).

A three-fourth inch wide by one-fourth inch thick by three inch long steel plate to simulate the anchor was inserted at distances of six and twenty-four inches down from the top of the roller array. A one-eighth inch diameter stainless

steel cable was connected to the anchor plate and led up through the roller array at the required angle for each test.

The steel cable was led through a series of pulleys in a frame located above the test tank to a hydraulic cylinder having a twenty-one inch stroke. This hydraulic cylinder was actuated by a manually operated hydraulic hand pump. Connected between the hydraulic cylinder and the pullout cable was a Baldwin-Lima-Hamilton load cell. Three different load cells having capacities of 100, 200 and 2,000 pounds were used depending upon the load required to withdraw the anchor plate. The load cell was connected to a constant-speed Minneapolis-Honeywell Visicorder to record continuously the pullout load directly in pounds. Figure 1 shows a drawing of this apparatus.

A Nikon F 35 mm camera with a battery operated film drive was set on a tripod squarely in front of one of the plexiglas faces of the roller tank. Photographs of the roller array and the anchor plate were taken through the plexiglas face at desired intervals of anchor pullout to record roller displacements.

Each test was performed in the following manner:

One of the plexiglas faces of the tank was removed to allow the ends of the rollers to be cleaned with a volatile solvent. The array of rollers was arranged in a manner to secure a uniform packing and density over the entire volume. The top of the array was leveled.

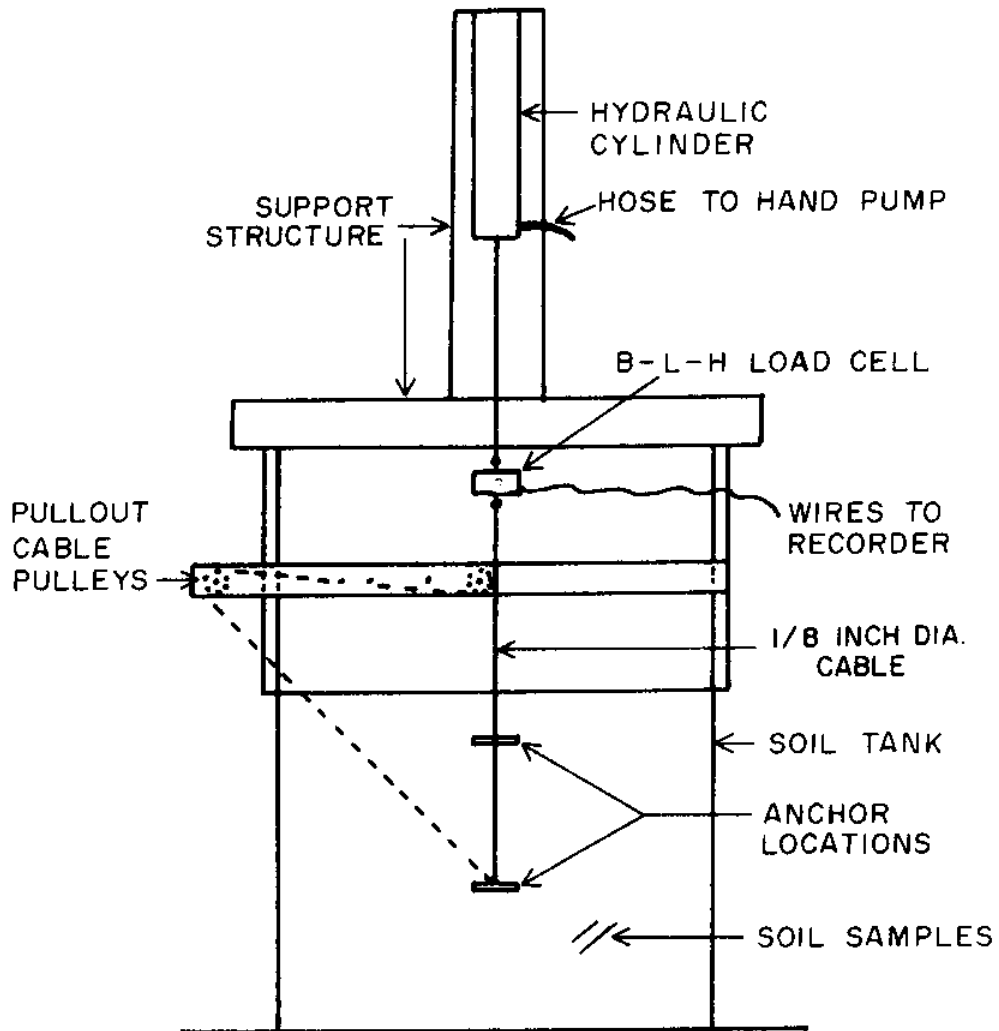


FIGURE 1 SKETCH OF PULLOUT TEST APPARATUS

The anchor plate and its attaching cable were inserted into the roller array at the desired distance down from the top and with the cable at the desired angle of inclination. The visible edge of the anchor plate was painted white and a grid of white lines, two inches on centers both ways, was marked on the exposed ends of the rollers. The plexiglas face of the tank was then reinstalled and secured.

Needless to say, all of the above operations, done while the roller array was exposed, were performed by skilled people in a most careful manner. A pile of 150,000 rollers accidentally spilled on the laboratory floor is a great incentive to careful work.

The pullout cable was connected through the load cell to the hydraulic cylinders. The Visicorder was warmed up and started. The calibration of the load cell was checked and the test began by manually pumping the hydraulic cylinder. The pumping rate was constant for all tests at 22 strokes per minute. The displacement of the anchor was 0.045 inches per stroke or two and three-fourths inches per minute.

In most tests, the maximum pullout load occurred at displacements of less than one inch but pullout was continued until the anchor reached the surface of the roller array.

Photographs of the displacements of the rollers and anchor plate were taken at times when it was deemed necessary so that

a complete record of the particle (roller) movements could be recorded. The number of photographs taken varied between 20 and 35 for each test.

Three-dimensional Tests

The three-dimensional tests were conducted in soil materials contained in standard soil tanks as used at the Terramechanics Laboratory. These tanks are made of heavy gauge steel, are cylindrical in shape, and are 30 inches in diameter by 42 inches high. The loading frame containing the pullout cable pulleys, hydraulic cylinder, and hydraulic hand pump used for the previously described two-dimensional tests was arranged over the top of the soil tank.

The material used for the sand tests was commercially available air-dry Ottawa sand 0.1 mm to 0.6 mm. It was placed in the soil tank such that it was at its maximum density. The method of placement to achieve this density had been developed over the past few years by the personnel at the Terramechanics Laboratory and had been used for many successful penetration tests. Murff and Coyle (38) describe this technique as follows:

It was found that compacting 4-5 inch layers with repeated prodding of a concrete vibrator resulted in a target very near maximum density. Pouring the dry sand through a screen held a fixed distance above the soil surface resulted in a very loose configuration. It was found that the average density of the target could be controlled in both cases within a range of +2%.

The properties of the dense dry sand targets were:

Bulk Density	110 lbs/ft ³
Dry Density	110 lbs/ft ³
Moisture Content	0 %
Degree of Saturation	0 %
Void Ratio	0.5
Unconfined Compressive Strength	0
Angle of Internal Friction	34.2°

As the soil sample was built up in the soil tank, the anchor plate was placed at the proper level, the pullout cable was held at the desired angle, and the layers of soil were continued to the top of the tank. The top of the soil sample was struck off level with the tank top.

For the tests run in submerged sand, the same Ottawa sand was used and was placed in the dense state in the same manner as for the dry tests. Upon completion of the placement of the anchor plate and pullout cable and leveling of the top of the soil sample, submergence was begun. This was accomplished in the same manner as had been developed by the Terramechanics Laboratory staff. A fresh water line was attached to an inlet at the very bottom of the soil tank. The water was turned on at a very slow rate. This slow rate of water entry insured that all air in the voids of the sand was expelled as the water level rose. It took from four to six hours for the water level

to reach the top of the sand sample. It was held at this level until the pullout test was completed.

The marine sediment tests were performed in the same soil tanks as were the sand tests. The marine sediments were provided by the Geological Oceanography Division at Texas A&M University. They had been secured from the Gulf of Mexico during previous sampling cruises of the R/V Alaminos. They were stored in the sample containers in which they had been gathered and had been submerged during storage. The sample containers were square aluminum tubes, 12 inches by 12 inches by 36 inches high. Six of these samples were provided.

The marine sediment samples were removed from the sample containers and were carefully placed in the 30 inch diameter soil tanks. Each layer of sediments was carefully kneaded as it was placed to avoid entrapping air to the greatest extent possible. The submergence which had been observed during storage was maintained during testing.

The manner of placing the anchor plates for this series was different from that used during the sand tests. In the weak, semi-fluid clay samples, the anchor plates were simply pressed down through the clay to the desired depth by hand and held in that position until the angle of pullout cable inclination was made. Then the clay was manually kneaded into place over the plate and cable back up to the surface, which was struck off level with the tank top.

The properties of the marine sediments were measured as:

Miniature vane shear test (1/2" vane)	63.1 PSF
Water Content (% dry weight)	136.6
Liquid Limit	128.
Plastic Limit	49.

These properties are typical for the surface sediments that cover extensive areas of the floor of the Gulf of Mexico basin as shown by Figures 70 and 74 of the report by Nowlin, Bryant, and Thompson (39). An excellent summary of the geotechnical properties of Gulf marine sediments is given by Bryant, et al (6).

The procedure of test performance of these tests was the same for all three materials. The pullout cable was connected through the load cell to the hydraulic cylinder. The test was commenced as in the two-dimensional series and was continued until the anchor plate broke the soil surface. The pullout force was recorded and photographs were taken of the soil sample surface at intervals as evidence of failure was shown there.

The anchor plate used in these tests was made of steel, was three inches in diameter, and was one-fourth inch thick. The holes drilled in it for the eccentric load application are shown in Figure 2. Holes not being used were closed with flush threaded plugs during all tests. The same one-eighth inch diameter cable was used for pullout as in the previous test series.

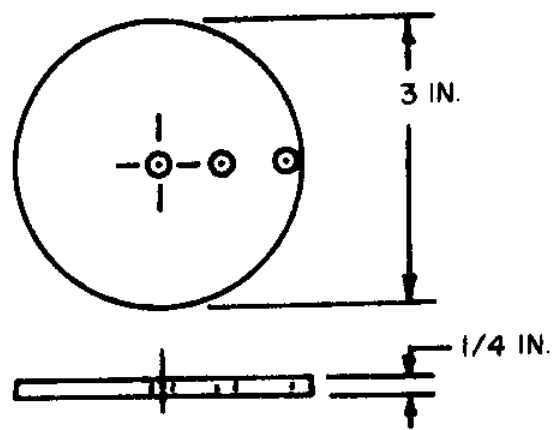


FIGURE 2 ANCHOR PLATE

EXPERIMENTAL RESULTS

The definition drawing of the nomenclature used in the laboratory test phase of this study is shown in Figure 3.

The observed pullout force values from the 40 laboratory tests performed in this study are shown in Table I.

Over two hundred and fifty 35 mm photographs of the roller displacements during anchor pullout tests in the two-dimensional series were taken. These photographs were enlarged to the maximum format that would include all of the displacements and were printed on eight inch by ten inch paper. Care was exercised during the printing of the photographs of each series so that the distance from the negative to the printing paper was held constant. This insured that each photograph of a series had the same linear scale as the others, allowing direct roller displacement comparisons. A typical photograph is shown in Figure 4.

The comparison of observed data for roller bearing maximum pullout forces against dry sand maximum pullout forces as they are influenced by inclined angles of load application and depth of burial is shown in Figure 5. The comparison of the same maximum pullout forces as they are influenced by load application eccentricity and depth of burial is shown in Figure 6.

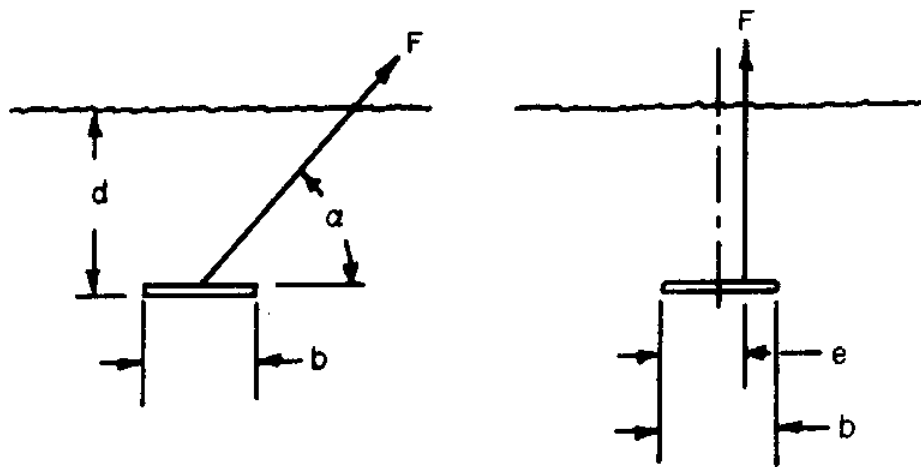


FIGURE 3 DEFINITION SKETCH

TABLE I LABORATORY TEST DATA

d/b	α (°)	e/b	Roller Bearings		Dry Sand		Submerged Sand		Marine Sediment	
			Test No.	F (lbs)	Test No.	F (lbs)	Test No.	F (lbs)	Test No.	F (lbs)
2	90	1/2	1	6	11	18	21	18	31	22
2	67-1/2	1/2	2	8	13	28	23	26	32	24
2	45	1/2	3	9	15	32	25	28	33	24
8	90	1/2	4	110	12	365	22	230	34	28
8	67-1/2	1/2	5	120	14	455	24	325	35	40
8	45	1/2	6	165	16	685	26	195	36	40
2	90	3/4	7	6	17	22	27	14	37	8
2	90	1	8	4	19	12	29	8	39	6
8	90	3/4	9	85	18	220	28	280	38	22
8	90	1	10	75	20	180	30	165	40	14

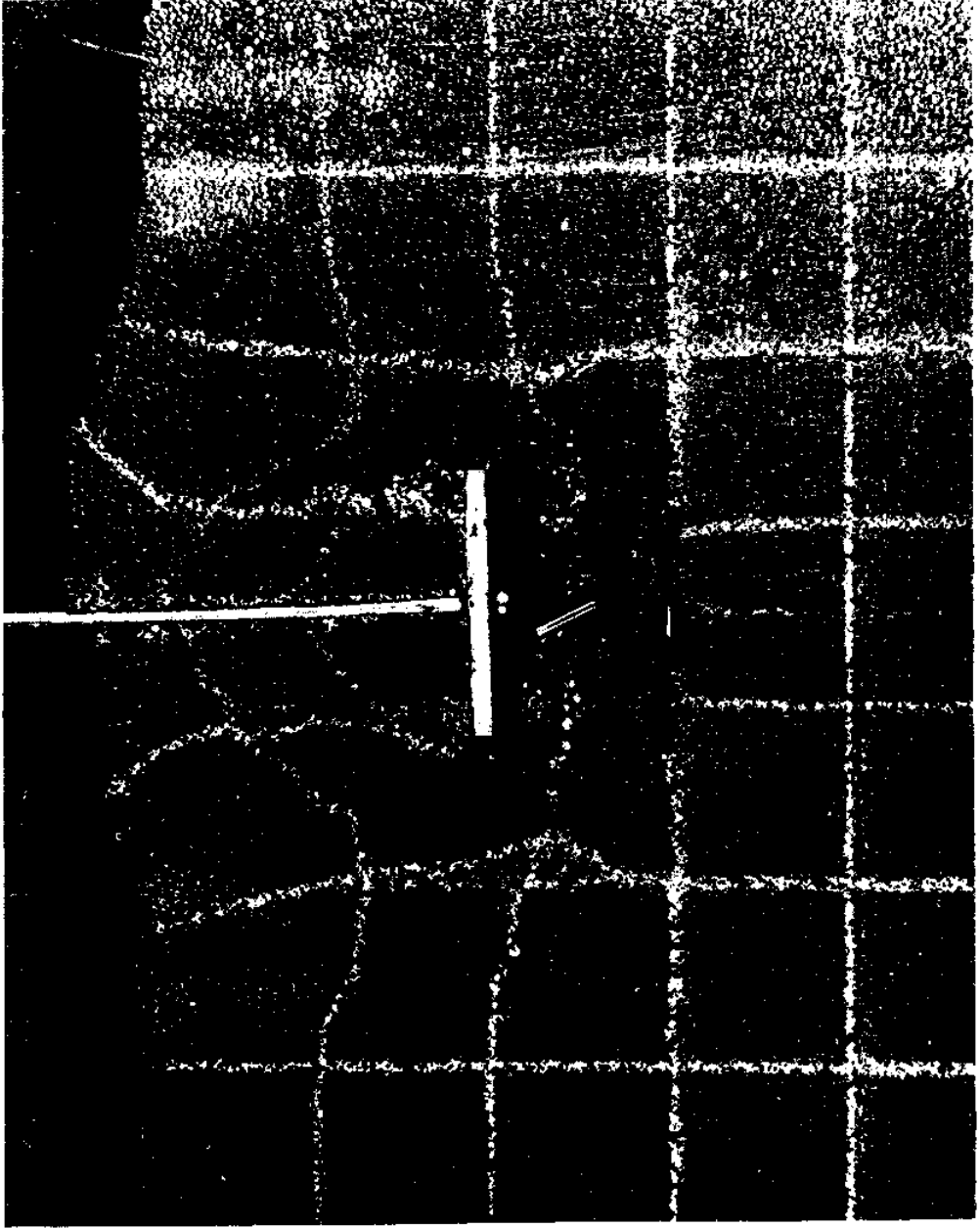


FIGURE 4 - PHOTOGRAPH OF TYPICAL TWO-DIMENSIONAL ROLLER DISPLACEMENTS

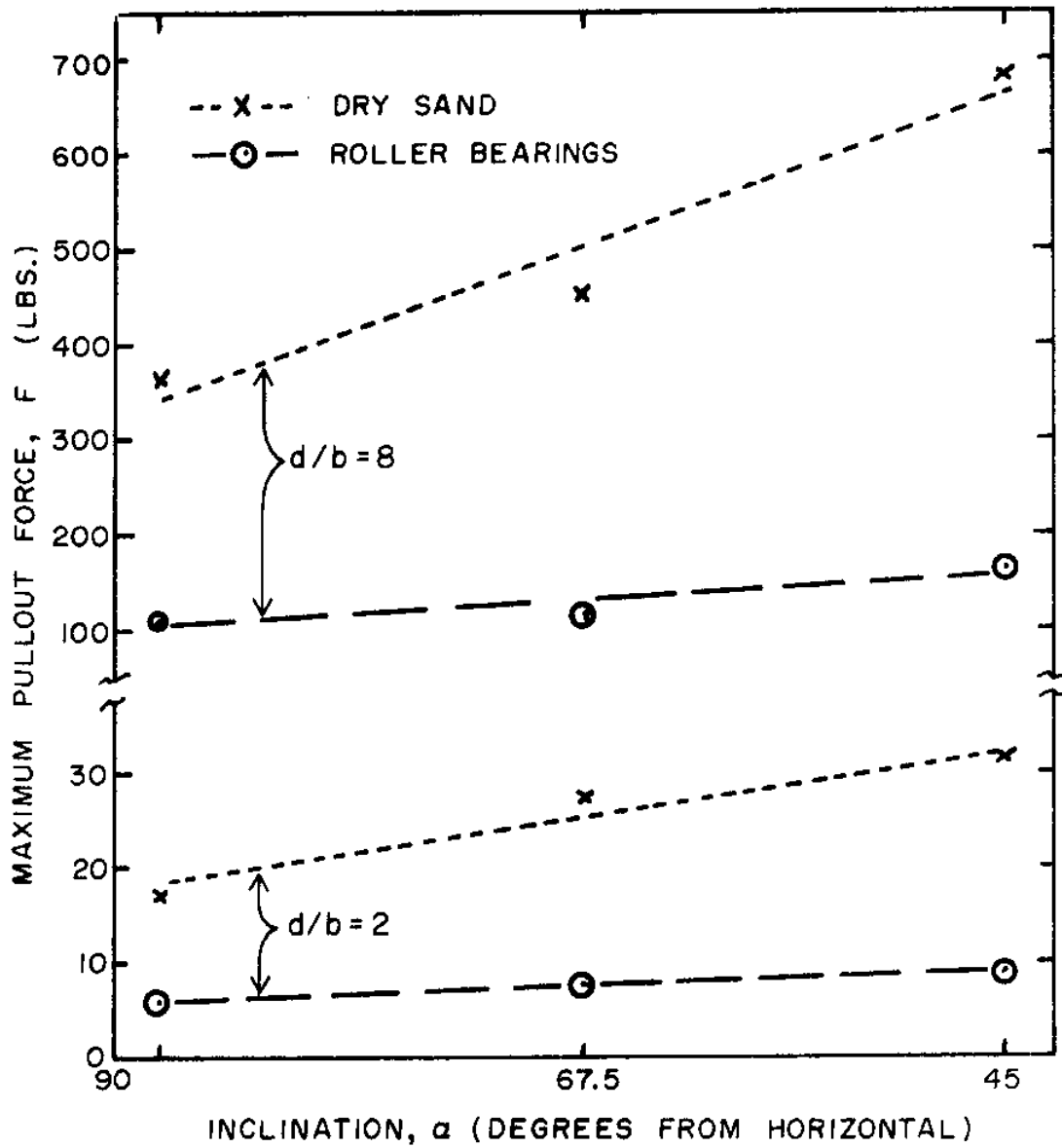


FIGURE 5 PULLOUT FORCE vs INCLINATION, ROLLER BEARINGS AND DRY SAND

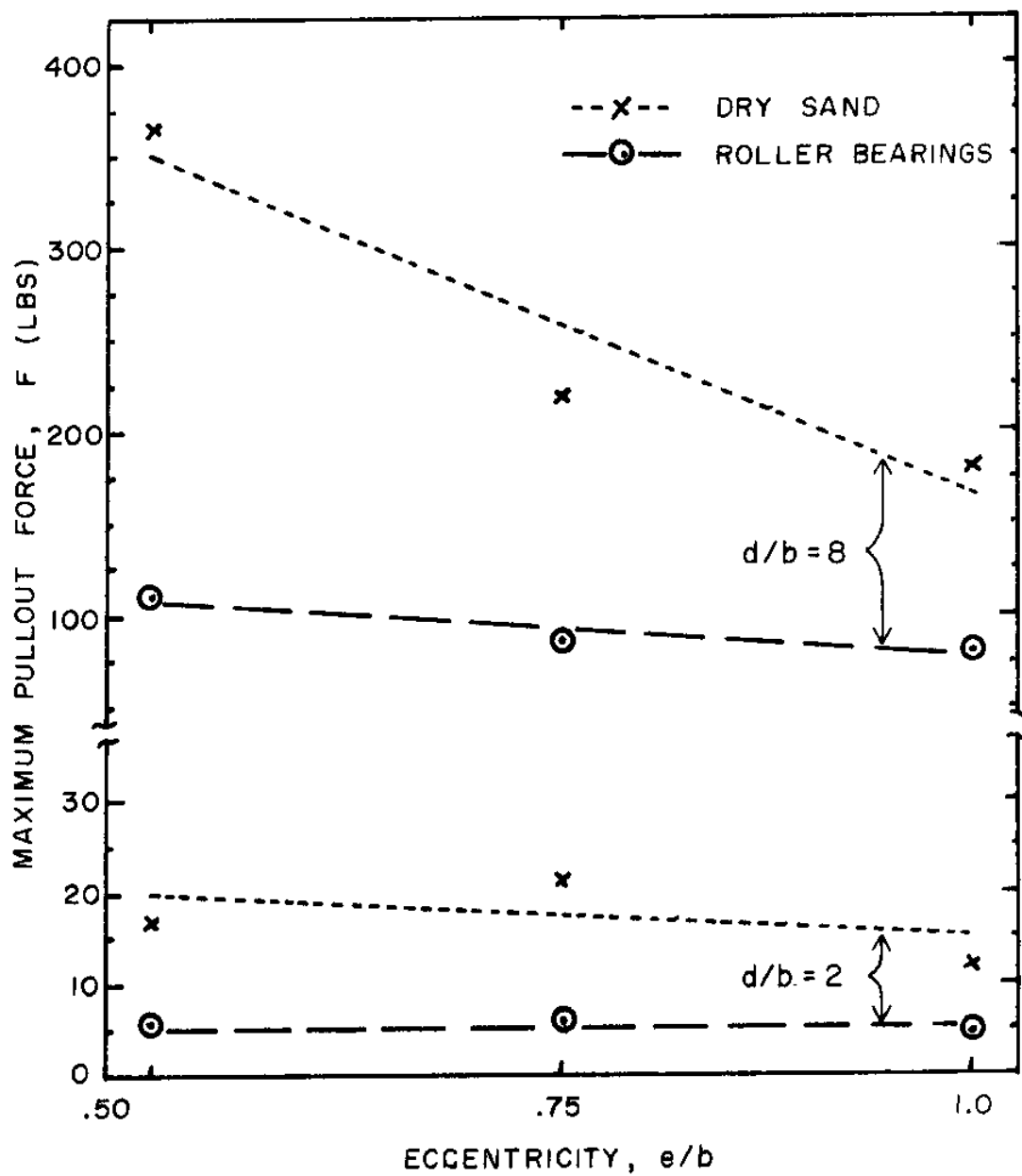


FIGURE 6 PULLOUT FORCE vs ECCENTRICITY, ROLLER BEARINGS AND DRY SAND

The observed data showing maximum pullout forces for all three types of soil tested (dry sand, submerged sand and marine sediments), as they are influenced by load application inclination and depth of burial are plotted on Figure 7. The comparison of the same maximum pullout forces as they are influenced by load application eccentricity and depth of burial is shown in Figure 8.

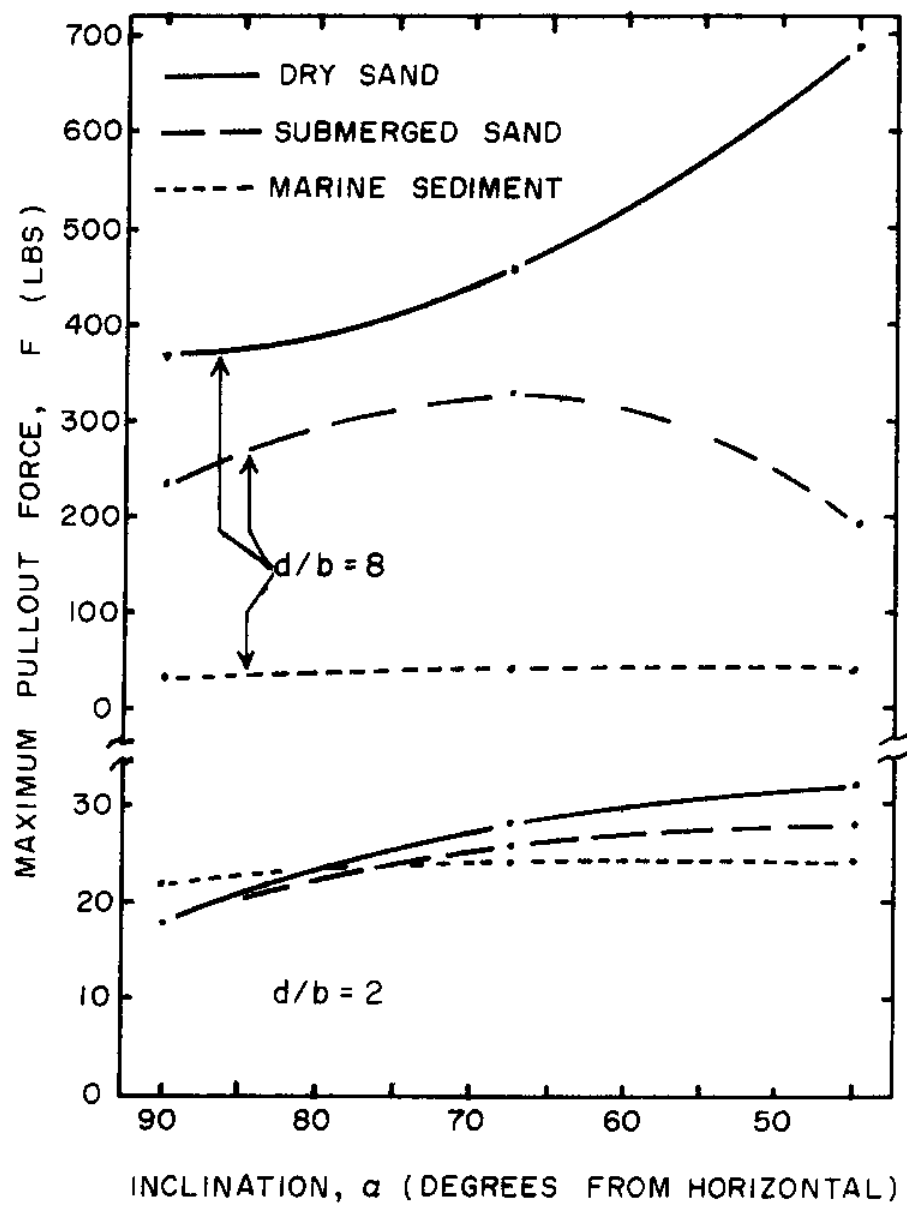


FIGURE 7 SOIL EFFECT ON PULLOUT FORCE VS INCLINATION

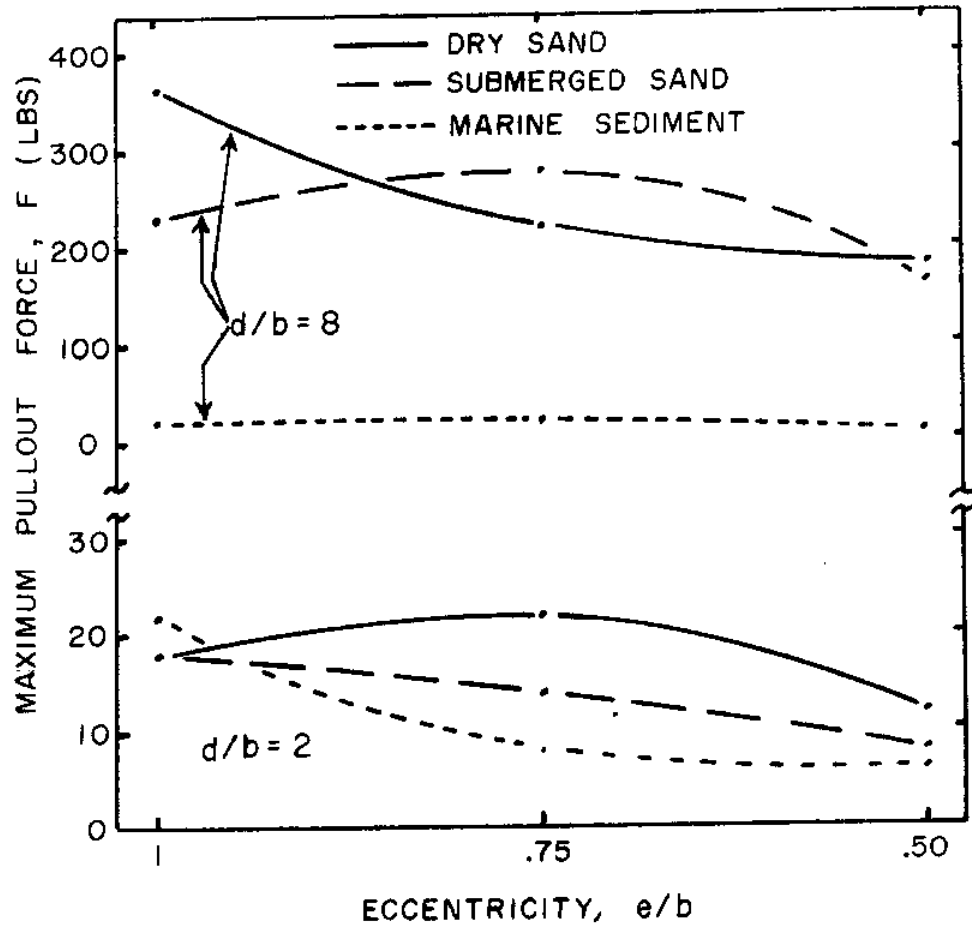


FIGURE 8 SOIL EFFECT ON PULLOUT FORCE VS ECCENTRICITY

DISCUSSION OF RESULTS

Two-dimensional Tests

The laboratory tests into the two-dimensional array of steel roller bearings were performed only for the purpose of visually observing the displacements of individual particles of a simulated, dense, granular, cohesionless soil during anchor pullout. Although the experimental technique of using steel roller bearings to simulate such a soil had been used in the past (8) and the successful results achieved had been demonstrated (9), it was felt desirable to see if such a simulation technique was applicable to anchor pullout studies.

Justification of experimental technique. To verify the validity of this technique, the maximum pullout load required in each of the roller bearing tests was recorded and was compared with the same values obtained from the dense, dry Ottawa sand tests in three dimensions. Figures 5 and 6 show this relationship as affected by load application inclination, load application eccentricity, and depth of burial. In Figures 5 and 6, best-fit straight lines have been drawn between the observed data points, since it is the trends of the data that are being compared to evaluate the relationship.

Figure 5 compares the maximum pullout load recorded against the load application inclination angle for depth of burial (d/b) of 2 and 8 for both materials. At both depths of burial, the

maximum pullout forces increase as the load application inclination angle goes from 90° (vertical) to 45° for both materials. The force-inclination line is steeper for dry sand in both cases, but the important thing is that the trends for both materials are in the same direction thus indicating a similarity. Also, the ratios of the average values of the force-angle lines for both materials are in good agreement at both depths, in this case being 3.6 for $d/b = 2$ and 3.8 for $d/b = 8$.

Figure 6 compares the maximum pullout load recorded against the load application eccentricity (e/b) for depths of burial (d/b) of 2 and 8 for both materials. At both depths of burial, the maximum pullout force for both materials decreases as the load application eccentricity moves from the center of the anchor toward one end. The force-eccentricity line for dry sand is again steeper than that for the roller bearings. In this case, the ratios of the average values of the force-eccentricity lines for both materials are identical at a value of 2.9 for d/b of 2 and 8. It again appears that the action of roller bearings during pullout tests is similar to that of dry sand.

Based on the author's previous successful experience with this experimental technique and on the laboratory pullout test results discussed above, it appears that the use of an array of roller bearings to simulate the particle actions of a granular, cohesionless soil (dry sand) is justified.

Particle displacement. The number of photographs taken of the particle (roller) displacements in each two-dimensional test averaged about 25. The method chosen to best analyze the data from each test was to select four photographs showing a sequence of anchor displacement and study them. Since the pullout load-time curves recorded for each test indicated that in all tests the maximum pullout load had occurred before the anchor had been displaced two inches, it was only necessary to examine those photographs showing up to that amount of anchor displacement. In most cases, photographs of greater displacements were included to show other interesting particle motions that occurred after the initial failure.

To delineate the amount of particle motion in each of the sequential photographs, a drawing on transparent film of the anchor in place and of each of the grid of lines that had been placed on the roller bearing array was traced from the photograph taken immediately before each test. Since each photograph in each test sequence had been printed at exactly the same distance from negative to print, the scale from photograph to photograph was identical. The tracing from the first photograph could be placed over the next selected one in the sequence and by tracing the new positions of the grid lines, the displacements could be shown. The four tracings thus secured from each test series were placed on one figure for study. Each figure thus

prepared will be discussed in detail below.

Figure 9 shows the particle displacements of a vertical pullout at a shallow depth ($d/b = 2$). View A shows the formation of the heaved surface which began as soon as the anchor started to move. In a dense, granular, cohesionless material, this surface heave from a shallow pullout must occur with small anchor displacements since the nearby ground surface is a stress-free boundary. An open void (depicted in Figure 9 by a stippled area) is visible directly below the anchor plate. [It must be kept in mind while studying these results, that these are true two-dimensional representations of particle (roller) motions. That is, there are only two (vertical and horizontal) dimensions in the plane of the test. There is no dimension into the plane of the test (the roller array). In other words, this test can be thought of as a cross-section taken through a sand test when the cross-section has a thickness of only a single grain of sand.]

As the anchor displacement continues through Views B, C, and D, the extent of the shearing action (movement of one particle over another) associated with the pullout can be clearly seen. In View B, the vertical lines directly above the plate show little movement; indicating that up to that point, those rollers

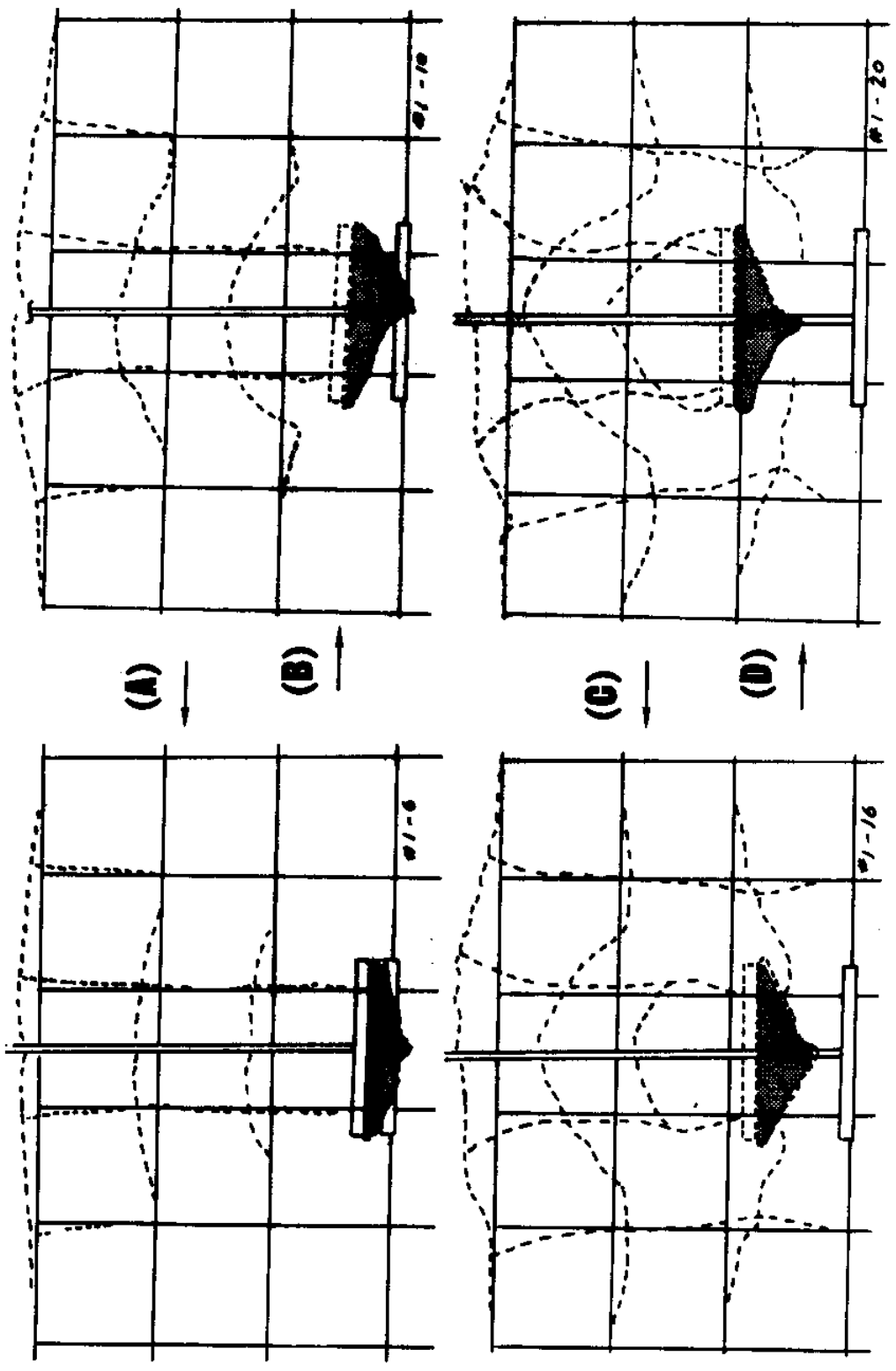


FIGURE 9 — ROLLER PULLOUT TEST NO. 1 - 90°, d/b = 2, e/b = 1/2

have been moving almost as a rigid body while the failure has been taking place out at the sides. Evident in this view is the inception of the downward movement (counterflow) of loosened (sheared) particles to occupy the space below the moving plate.

Figure 10 shows the effect on a shallow anchor of inclining the pullout force to $67\frac{1}{2}^{\circ}$ from the horizontal. Again, surface heave occurs at small displacements. An open void occurs below the anchor plate, but it is not as large as in the vertical pullout case. The counterflow (downward) of particles is much greater than in the previous case and is accentuated on the less-stressed side. The vertical lines remain fairly vertical even into View C, but the inclined pull is causing them to be displaced to one side. A greater area of the particle array is being affected by the inclined pullout than was in the vertical case; indicating a greater resistance to pullout.

The fact that the anchor plate remains almost horizontal through all four views is of particular interest. As will be seen later, this is not the phenomenon observed in the more inclined or in the deep burial cases.

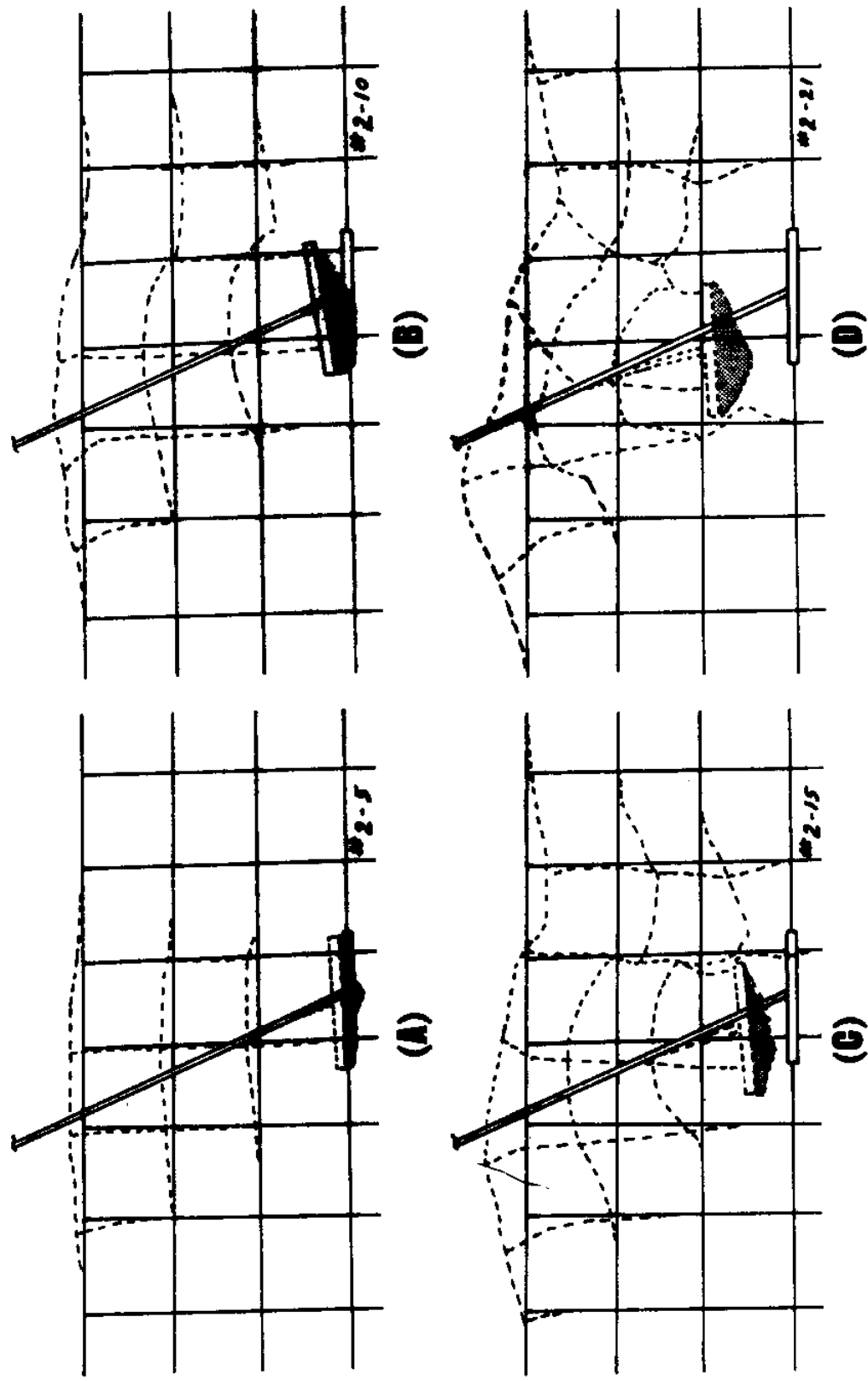


FIGURE 10 — ROLLER PULLOUT TEST NO. 2 - $67\ 1/2^\circ$, $d/b = 2$, $e/b = 1/2$

Figure 11 illustrates the effect of decreasing the pullout angle to 45° . The rigid body type motion of the material directly in line with the anchor plate still remains. The counterflow occurs early in this event and is almost totally restricted to the less-stressed side. The open void is even smaller than previously, indicating the influence of gravity on the counterflow. The attitude of the plate with respect to the line of action of the pullout force has changed in all views. In View D, the plate is normal to the force line.

The first deep burial test is shown in Figure 12, a vertical pullout. Surface heave is evident in View A when only a small anchor plate displacement has occurred. This indicates that in the dense simulated material being studied there is little compression occurring. However, as can be seen in Views B, C, and D, this early surface displacement was not continued and failure by counterflow around the plate occurred. The initial surface heave did not increase again until the anchor plate was quite near the surface. (However, observations of the surface of the later pullout tests in dry, dense Ottawa sand verified this early movement). The phenomenon of local shear failure is clearly shown in this sequence. The maximum load was reached quite quickly in this test, at less than one-half inch plate

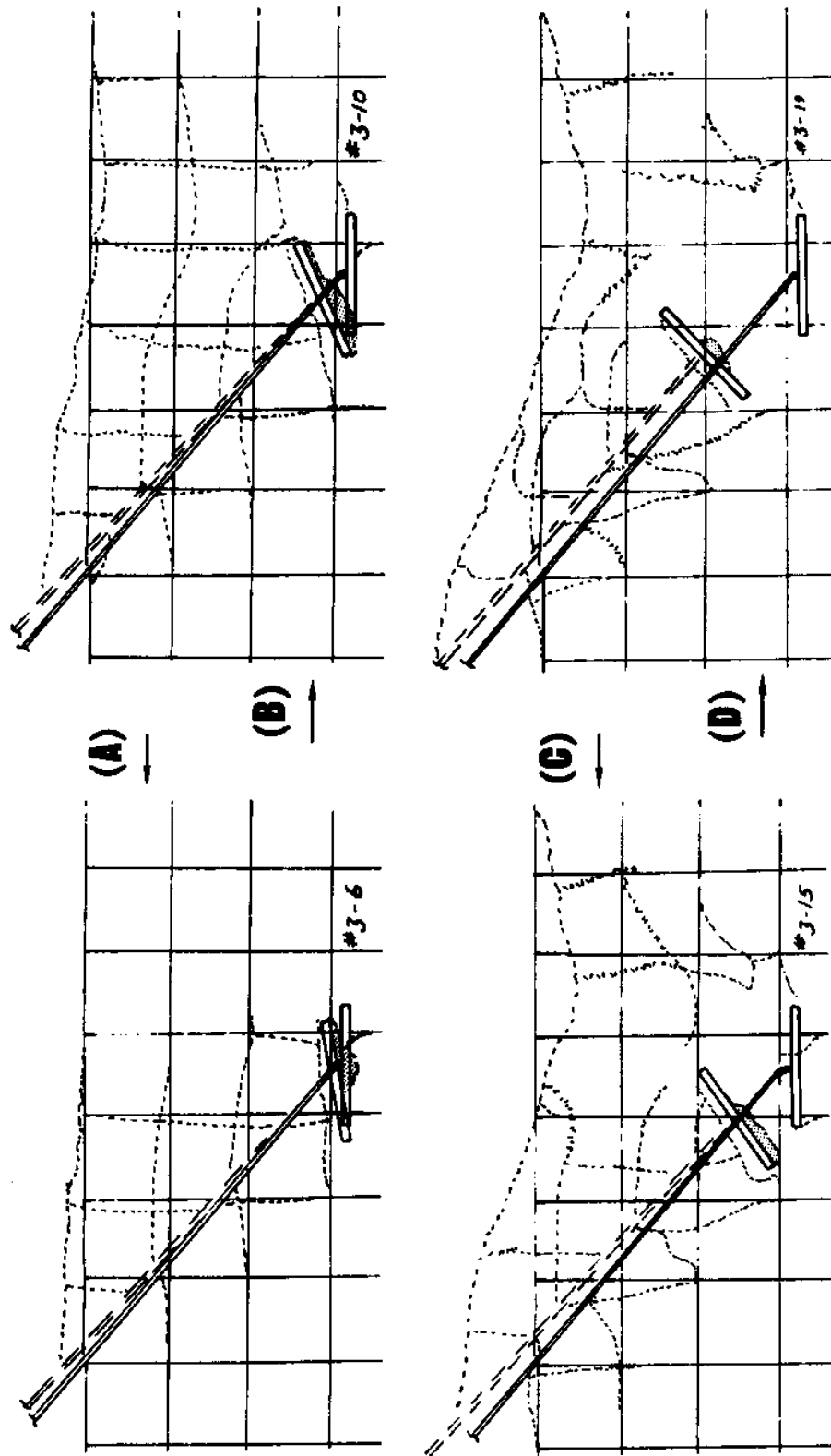


FIGURE 11 — ROLLER PULLOUT TEST NO. 3 - 45°, d/b = 2, e/b = 1/2

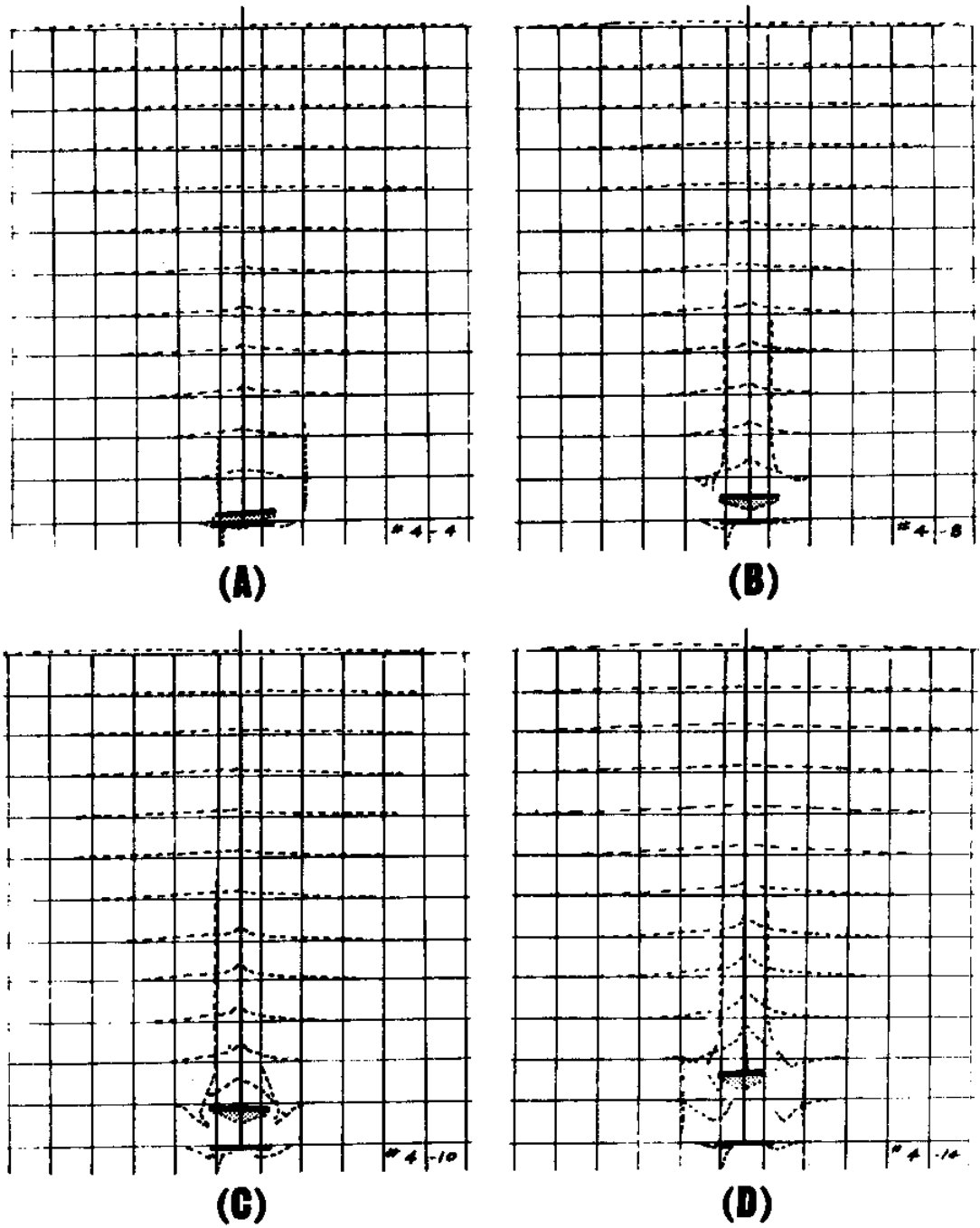


FIGURE 12— ROLLER PULLOUT TEST NO. 4 - 90°,

$$d/b = 8, e/b = 1/2$$

displacement. Then, when the local shear failure mode began operating, the load gradually decreased as the displacement continued. In Views C and D the "soil point", which Prandtl postulated in his bearing capacity theory and which is observed in foundation failure, pile driving, and projectile penetration, has formed directly above the anchor plate and is being carried upwards with it. An open void still remains below the ascending plate, even in this cohesionless material with a much greater overburden pressure.

A change in the angle of the line of action of the pullout force to $67\ 1/2^\circ$ from the horizontal causes the displacements shown in Figure 13. The occurrence of an early surface heave is the same as in the previous test, but, in this case, it is restricted entirely to the weaker side of the anchor plate. Unlike the same inclination in the shallow-buried test (Figure 10), the anchor plate turns to a position normal to the load line of action at a small displacement. Local shear failure is still the predominant mode, but the increase of surface heave is observed at smaller displacements than in the previous vertical test. Practically all of the particle movement occurs on the weaker side (right hand side in Figure 13) of the load line. The open void below the anchor plate remains but is much smaller in size. View D shows a phenomenon observed for the first time, that of

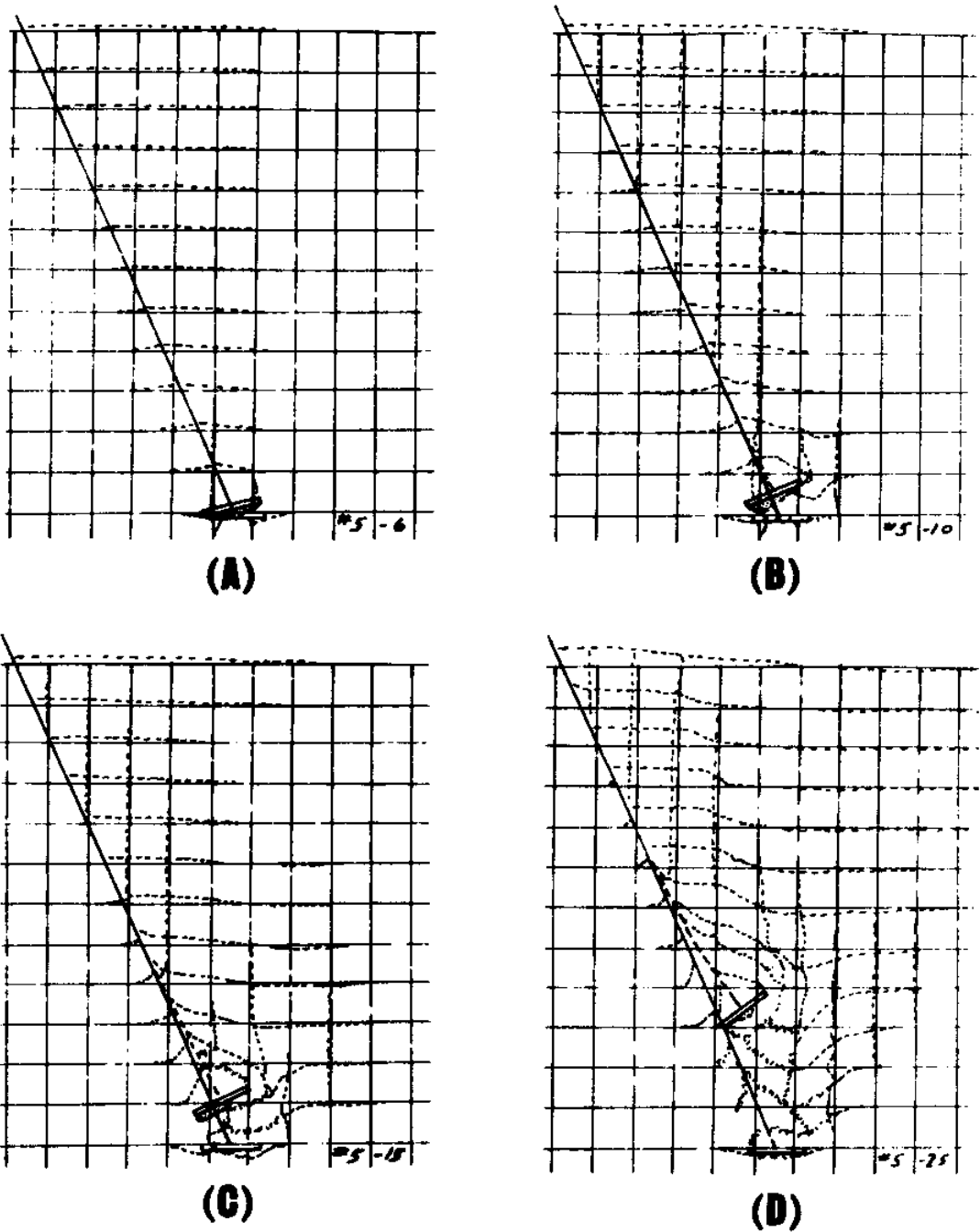


FIGURE 13 — ROLLER PULLOUT TEST NO. 5 - 67 1/2°

$$d/b = 8, e/b = 1/2$$

the displacement of the anchor plate horizontally toward the right or weaker side of the simulated soil mass. This movement could be expected and its occurrence under these deep burial conditions indicates that the greater overburden was necessary to increase the soil strength to the point where the compressed (left) side could force the plate over to the weaker side.

Figure 14, at 45° inclination, shows what might now be expected. The anchor plate quickly turns normal to the line of action of the load. The open void remains but is small. Very little displacement occurs on the stronger side. A larger amount of material is sheared during pullout. However, in this case, local shear is the major mode of failure; surface heave does not become evident until View C or until about two inches of displacement has occurred. By comparing View B of Figure 14 with Figure 13, B, it appears that counterflow of the particles was greater at the 45° angle, and thus may account for the increase in predominance of local shear at the small displacement stages.

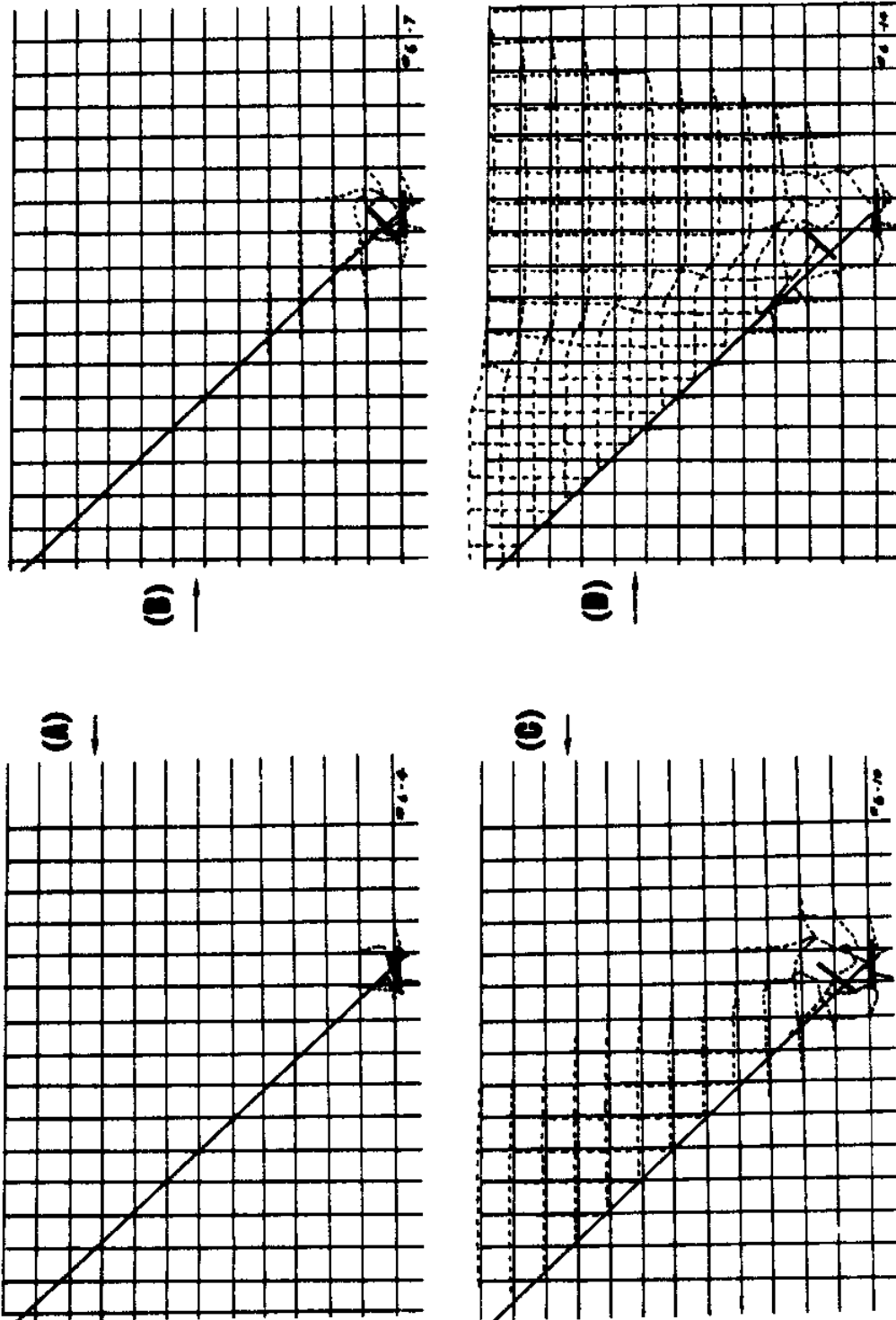


FIGURE 14 -- ROLLER PULLOUT TEST NO. 6 - 45°; $d/b = 8$, $e/b = 1/2$

Figure 15 is the first illustration that shows the effect of eccentricity (e/b) on the particle displacements during pull-out. In the shallow test depicted in Figure 15, the vertical pullout force point of attachment to the anchor plate is moved to a point midway between the middle and one end ($e/b = 3/4$). Comparing Figure 15 with Figure 9 shows several interesting differences due to the eccentricity increase. The anchor plate starts to move horizontally toward its shorter side at very small displacements and increases rapidly. Accordingly, most of the surface heave occurs on that side of the pullout cable and most of the counterflow occurs on the other side. A smaller amount of material is being sheared in the more eccentric test which would indicate a smaller pullout load required. An open void remains below the plate but it is very much smaller.

In Figure 16, the point of load application has been moved to the very edge of the plate. The plate pivots about its end opposite the point of load attachment. It still moves horizontally about the same amount as in the previous case. However, in this case, the counterflow completely occurs around the short end and the initial surface heave is greatly concentrated over the long end. Most noticeable is the greatly reduced amount of material that is sheared during the pullout. The open void still follows the upward moving end but is quite small due to the

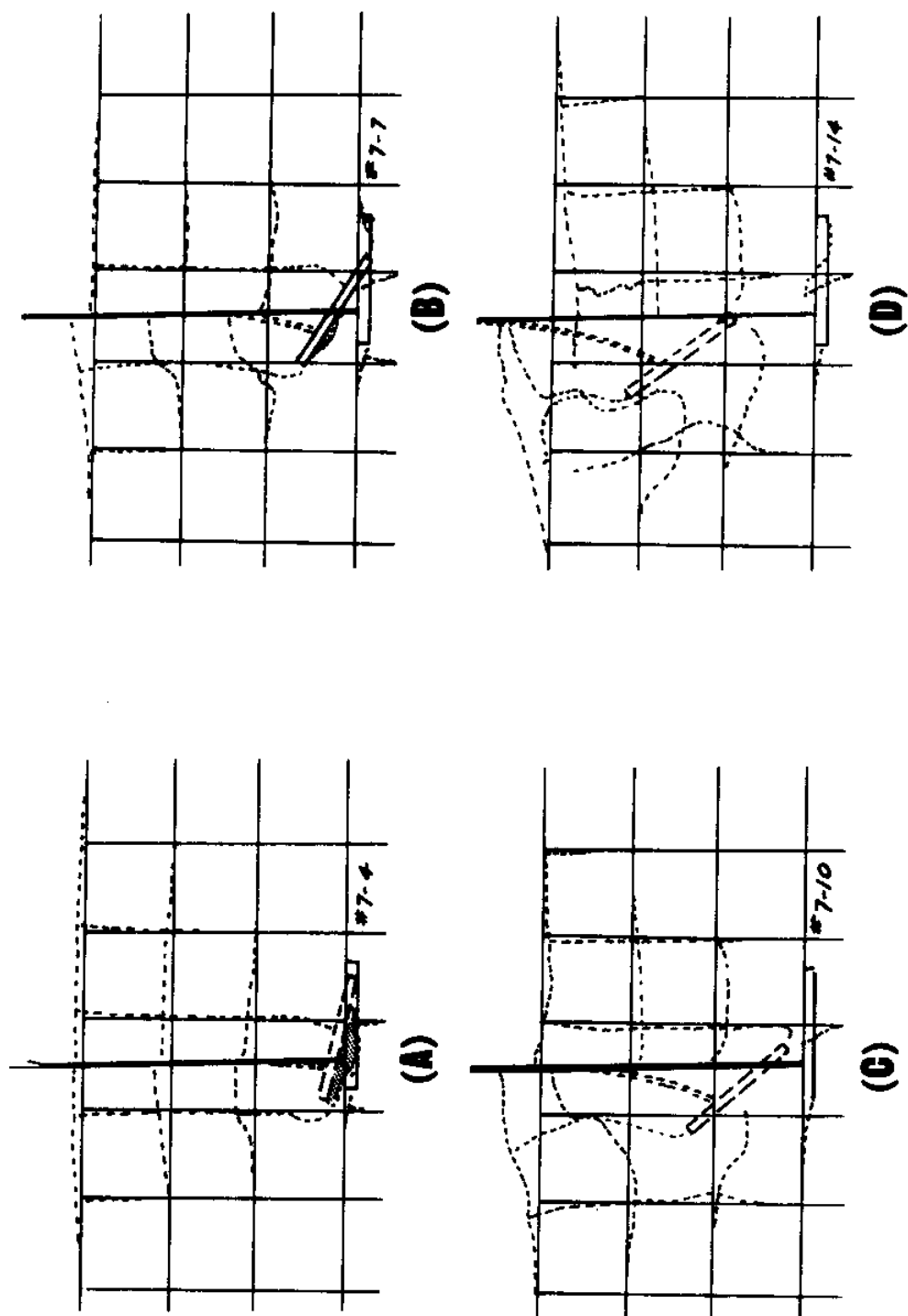


FIGURE 15 — ROLLER PULLOUT TEST NO. 7 - 90° , $d/b = 2$, $e/b = 3/4$

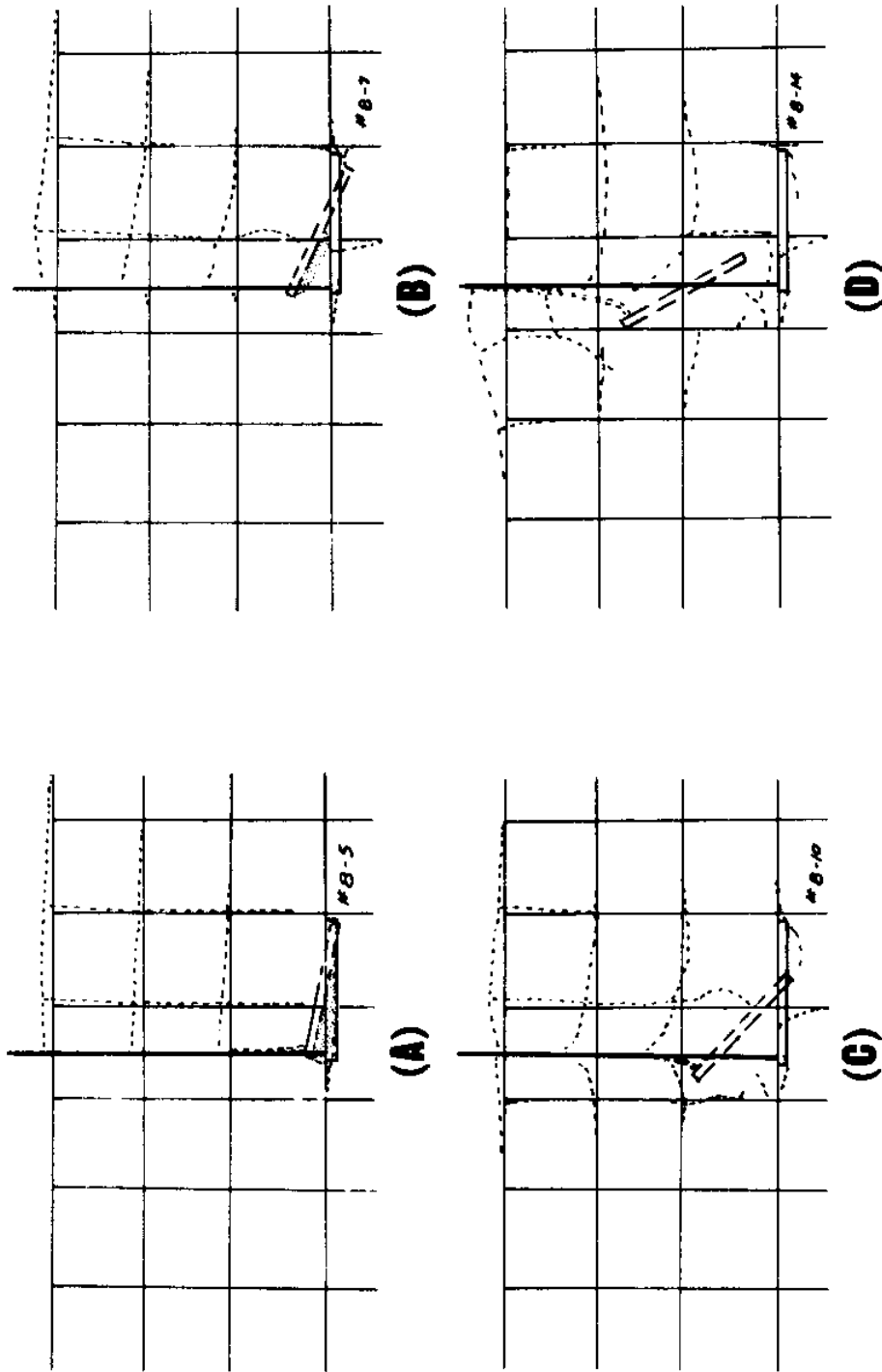


FIGURE 16 — ROLLER PULLOUT TEST NO. 8 - 90° , $d/b = 2$, $e/b = 1$

active counterflow around the attachment end.

Figure 17 shows the effect of an eccentricity of $e/b = 3/4$ on a deeply buried plate. As in the inclined, deeply-buried tests seen earlier, the principal mode of failure is local shear. Compared to Figure 12 which is a vertical mid-point pullout, the amount of material sheared appears to be smaller. As in Figure 15, the shallow-buried plate with $e/b = 3/4$, the deeply buried one moves horizontally while pivoting about its longer end. The amount of material sheared by the eccentrically loaded plate is appreciably less than in the mid-point loaded case. The counterflow is concentrated around the shorter end.

The end loaded plate shown in Figure 18 behaves about as would be anticipated now. The plate pivots about the long end. Counterflow occurs totally around the short end. Local shear is the failure mode and the amount of material sheared is quite small. The plate simply pivots to a near-vertical position and moves upward.

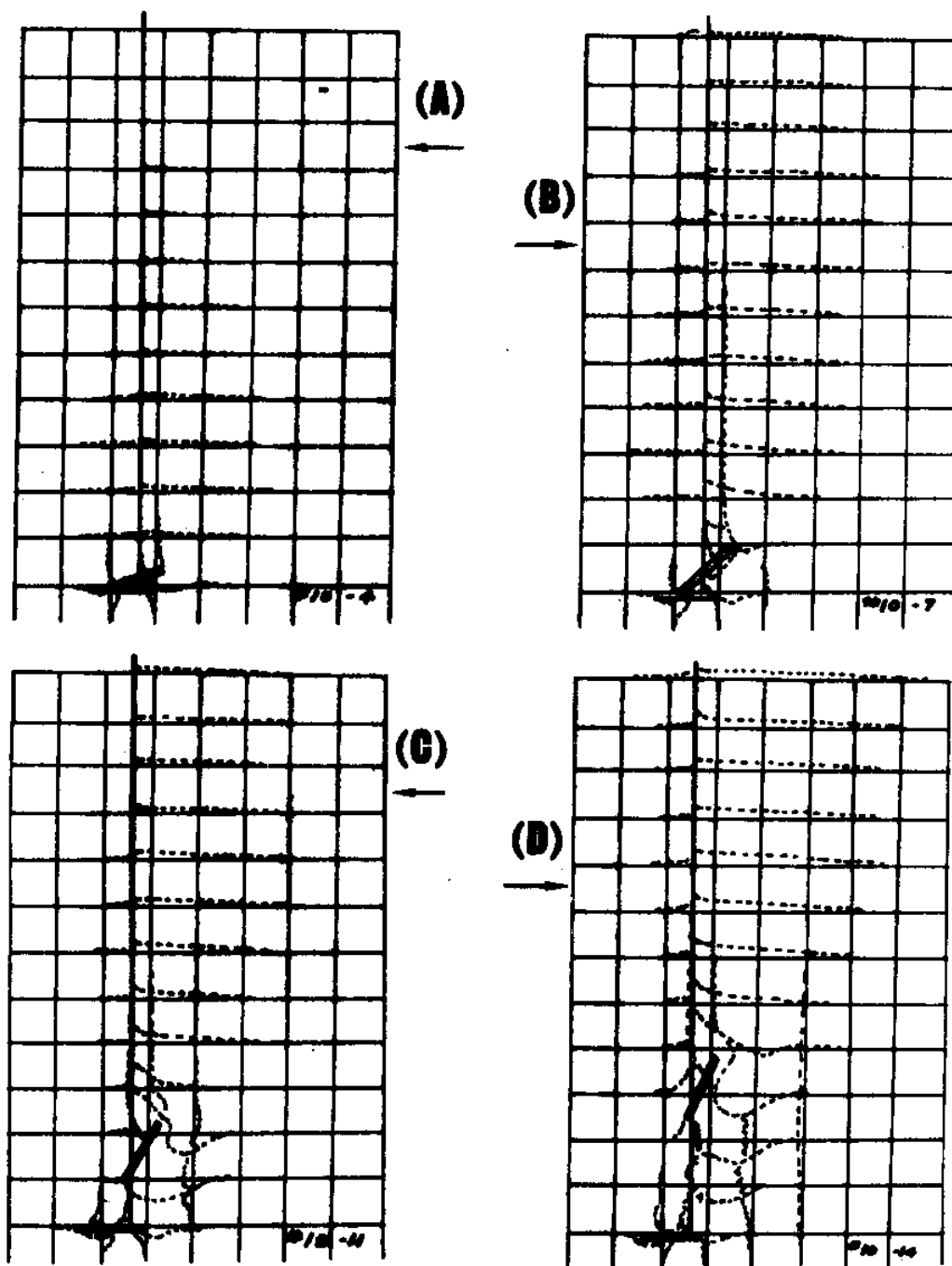
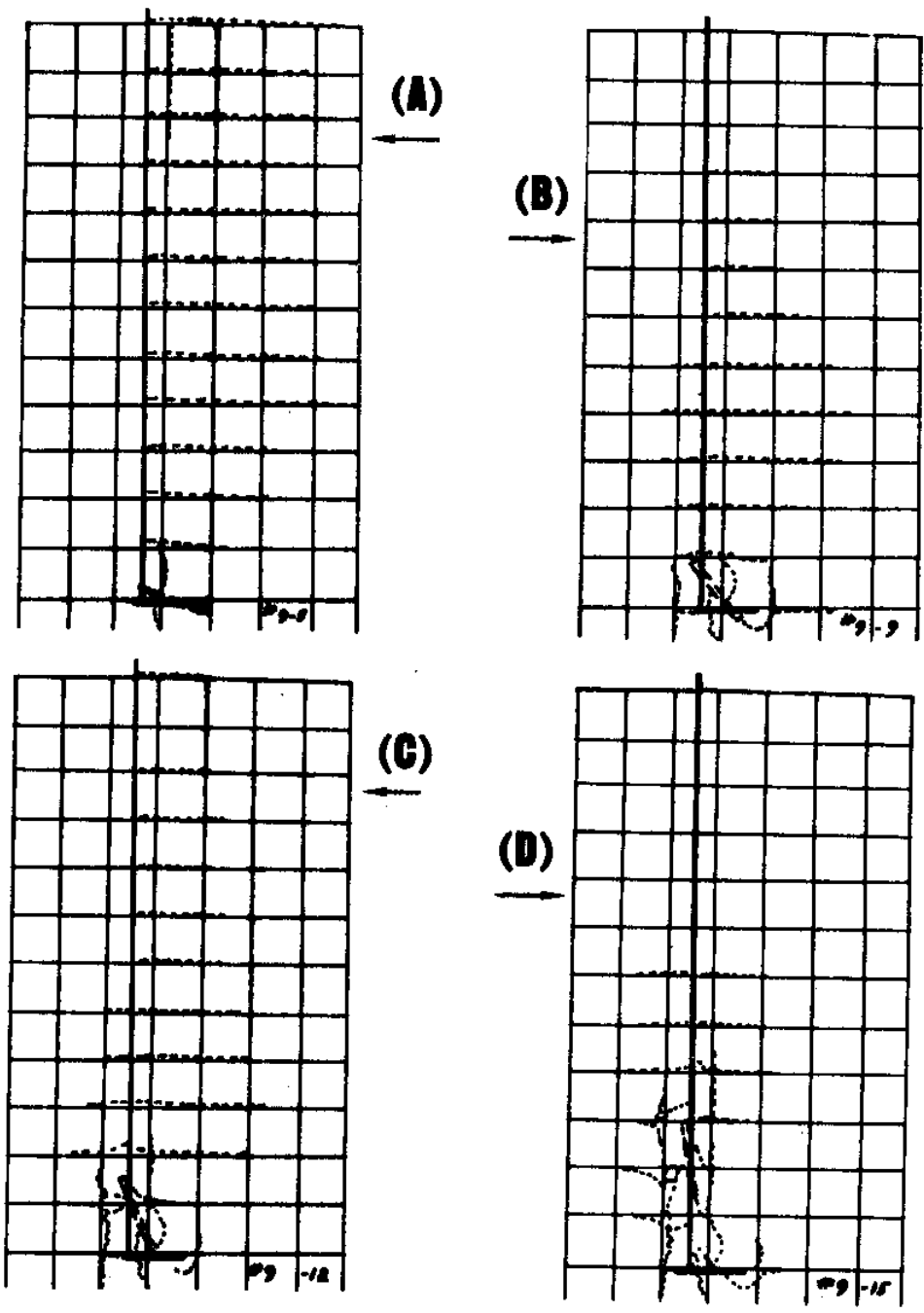


FIGURE 17— ROLLER PULLOUT TEST NO. 10 - 90°,

$$d/b = 8, e/b = 3/4$$



**FIGURE 18 – ROLLER PULLOUT TEST NO. 9 - 90°,
d/b = 8, e/b = 1**

The analysis of the visual observations of particle displacements just completed has indicated some interesting relationships.

Considering the inclination of the pullout force in a dense, granular, cohesionless medium; as the angle moves from the vertical toward the horizontal, it appears that:

1. The amount of material being sheared increases which should result in an increase in pullout force required.
2. The anchor plate does not rotate to a position normal to the force line of action until the inclination angle reaches 45° in the shallow-buried case; but, in the deeply buried case, it rotates at an angle of $67\frac{1}{2}^\circ$.
3. Regardless of the inclination angle, general shear failure with extensive surface heave is the failure mode in shallow-buried anchors; while local shear is the failure mode in the deeply buried cases.
4. An open void appears below the plate at some time in all cases; but the extent of the void is lesser as the angles approach 45° , and is much smaller in the deeply-buried cases.
5. The downward counterflow of sheared particles is evident in all cases but its amount increases as the angle approaches 45° .
6. In the inclined pullouts, counterflow is accentuated on the weaker (upper) side of the pullout cable.
7. The amount of particle displacement is very much less on the lower side of the pullout cable indicating a highly stressed (compressed) condition as opposed to that on the upper (free-boundary) side. [In the case of soils containing water in their pores, this phenomenon could be quite important as will be seen later in the submerged sand tests.]

Considering the eccentricity of the application of the pullout force in a dense, granular, cohesionless medium; as the point of application moves from the middle to one end of the anchor plate, it appears that:

1. The amount of material being sheared decreases rapidly.
2. The anchor plate pivots about its longer end inducing a compressive load in the material under that end.
3. General shear is the failure mode of the shallow-buried cases; but local shear is the failure mode of the deeply buried cases.
4. Most of the counterflow occurs around the shorter end of the plate.
5. In the cases where $e/b = 1$, the plate quickly turns to a near-vertical attitude and continues to the surface with a minimum amount of particle displacement.

Three-dimensional Tests

The three-dimensional tests conducted for this study involved the use of three types of soil materials: (a) dry, dense Ottawa sand, (b) submerged, dense Ottawa sand, and (c) Gulf of Mexico marine sediments. The measured properties of these soils has been given earlier in this report.

Soil effects considering inclination. Figure 7 depicts the change in the magnitude of the maximum pullout force required as the angle of pullout force inclination varies from 90° to 45° from the horizontal for all three materials at two depths of burial, $d/b = 2$ and 8.

Study of Figure 7 reveals that in all materials, the deeper-buried cases required greater force to pullout the anchor regardless of inclination. In the dry sand material, this force increased almost uniformly as the angle approached the horizontal at both depths of burial. The ratio of the increase was about the same, being 1.77 for $d/b = 2$ and 1.87 for $d/b = 8$. The average maximum force required was 1900% higher in the deeply-buried case. In marine sediments, the force increase was quite linear and very slight. The ratio of the increase being 1.1 for $d/b = 2$ and 1.4 for $d/b = 8$. The average maximum force required was only 150% higher in the deeply buried case. In the submerged sand, the pullout force increased in an almost linear fashion at $d/b = 2$; but in the deeply-buried case, the pullout force showed an increase to an inclination of $67\frac{1}{2}$ degrees and then exhibited a lower value at 45° . Both of these pullout tests (at $67\frac{1}{2}^\circ$ and at 45°) were repeated to verify the values first obtained. In both of the repeated tests, the new values came within the range of experimental error. It can be postulated that the observed anomaly, i.e., the lower pullout force required at 45° , is a result of pore water dynamic effects on the strength of the sand being sheared. As seen in Figure 14, the roller pullout test for an inclination angle of 45° , almost all of the particle displacements occur on the upper side of the line of action of

the pullout force. The material on the lower side of this line is being highly loaded but because of the greater distance to the free boundary, failure is not occurring. This situation would mean that any free water in the pore spaces of the material on the lower side would be forced from its more pressurized state into an area of lower pressure. This lower pressure area would exist on the upper side of the line of action where the material is being actively sheared during withdrawal, since shearing of a dense, granular material results in an increase in its volume and void ratio (see Lambe and Whitman (24), page 131). The flow of the pore water, in this submerged case, from the compressed area into the sheared area would result in a buoyed situation in the sheared area and a decrease in its strength. This strength decrease would explain the lower value of pullout force measured.

From the study of Figure 7, it has been seen that marine sediments require much less force to pull out the plate anchor when $d/b = 8$ than is required in either of the two granular soils tested. At the shallow-burial depths tested, pullout force for the marine sediment material was much closer to that required for the granular materials but as the inclination angle approached 45° , the force required for the granular materials become appreciably greater than for the marine material. At both tested depths of burial, load inclination showed only a slight influence on the forces required to pull out a plate anchor embedded in

marine sediments.

Soil effects considering eccentricity. Figure 8 shows the change in the magnitude of the maximum force required to pull out the anchor plate as the point of attachment of the pull-out force moves from the center of the plate to one edge for all the materials tested at the two depths of burial, $d/b = 2$ and 8.

From Figure 8, it can be seen that at $d/b = 8$, dry sand exhibits in an almost linear relation, a decrease in force required as the attachment moves to the edge. Marine sediments exhibit a similar decrease but at a rate that is nearly flat. Again, the submerged sand shows an increase in force required followed by a decrease when the force attachment point is at the edge. Although the reason for this variation is not as clear as in the inclined case previously discussed, it must be due to the presence of free water filling the voids of the submerged sand.

At the shallow burial depth of $d/b = 2$, all of the withdrawal forces are less when attached to the edge than at the middle of the plate, but the dry sand shows an anomalous point at the value of $e/b = 3/4$. However, at this shallow depth, the forces being measured were small and the observed anomaly of this point could lie within the range of experimental error. Unfortunately it was not possible to repeat this test point.

The general conclusion can be drawn that the optimum point for attachment of the withdrawal force for its least value is

at the very edge of the anchor. However, for deeply buried anchors in the marine sediments tested, the data show that the decrease in maximum force required is not very large.

Dimensional analysis. The survey of the theoretical work that has been done in the field of anchor pullout forces did not reveal any development that considered anything other than a vertical, symmetrical force application. This study was intended to be an experimental approach to the problem of inclined and eccentric load application, so no theory development has been attempted. Instead, it was decided to use the technique of dimensional analysis to develop some encompassing dimensionless relationships that might prove useful in understanding the combined effects of the variables studied.

A dimensional analysis using the Buckingham π method was carried out and revealed the basic, independent, dimensionless π - terms to be: $\pi_1 = \alpha$, $\pi_2 = d/b$, $\pi_3 = e/b$, and $\pi_4 = F/b^2 S$. (The dimensional analysis and the calculation of these π -terms is shown in Appendix A.)

Each of the basic π - terms has a relationship to the other three; thus any two terms can be plotted against each other and result in a series of lines representing individual values of either of the two remaining π -terms. Most of the previous researchers had considered the dimensionless depth of burial term, d/b , as an important factor in anchor pullout performance. Accordingly, this π - term was chosen as the third variable for

the dimensionless plots made of the data obtained in this study. Since no previous data had been found by other researchers on tests into submerged dense sand, it was decided to omit the experimental results obtained from the tests using that material and only plot in dimensionless terms the data gathered in dry sand and marine sediments.

Figure 19 shows the dimensionless relationship that exists between $F/b^2 S$ and α for various values of d/b for dry sand. The curves shown for $d/b = 8$ and 2 are from the experimental data gathered in this study. One other previous study was found in which the effects of changing the angle of inclination of the pullout force was investigated. That work was done by Kananyan (22) at a d/b of 1.25 . Using the data he reported, the dimensionless force factor was plotted as shown on Figure 19. His data showed a slight increase in dimensionless force required as did the other two curves and it was located approximately in the correct relation to them.

Figure 20 depicts the relationship that exists between $F/b^2 S$ and the eccentricity term, e/b , for the dry sand data. Data from no other eccentrically-loaded tests could be found, so Figure 20 shows only the data from the experiments conducted during this study.

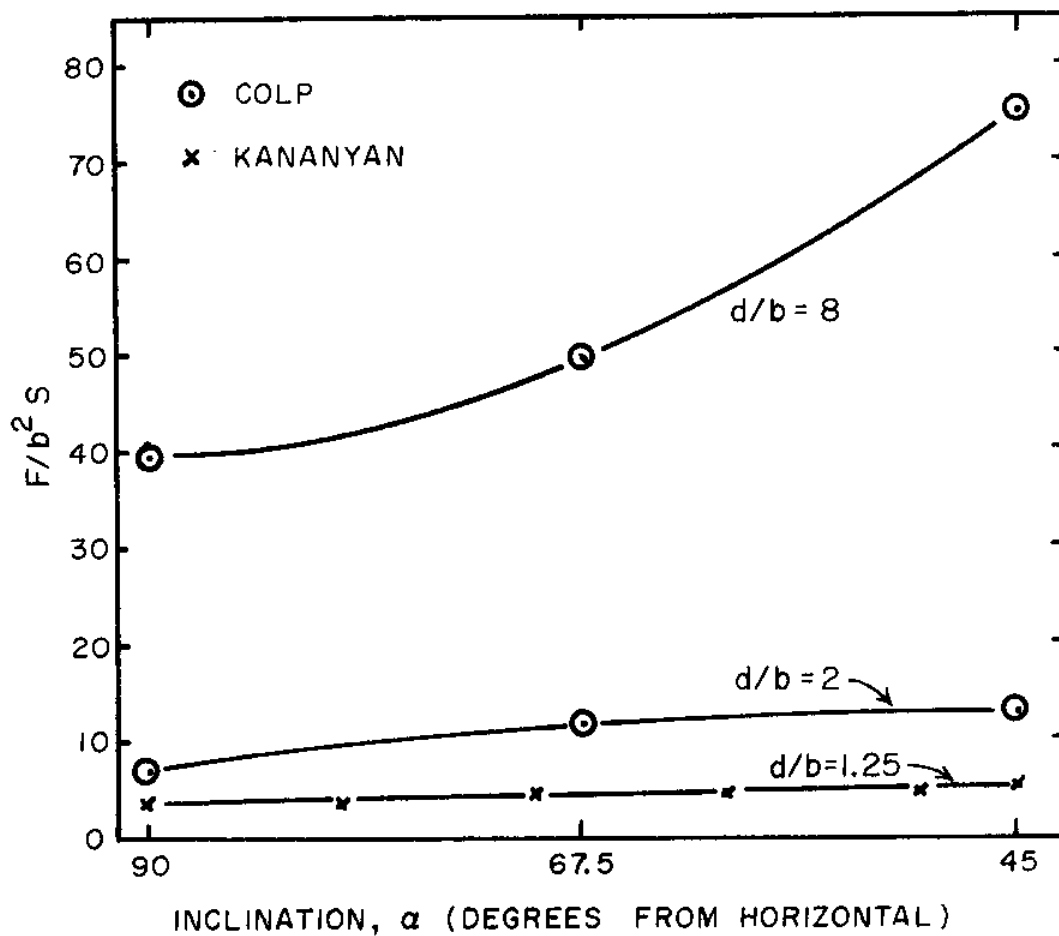


FIGURE 19 DIMENSIONLESS PULLOUT FORCE TERM vs DIMENSIONLESS PULLOUT CABLE INCLINATION FOR DRY SAND

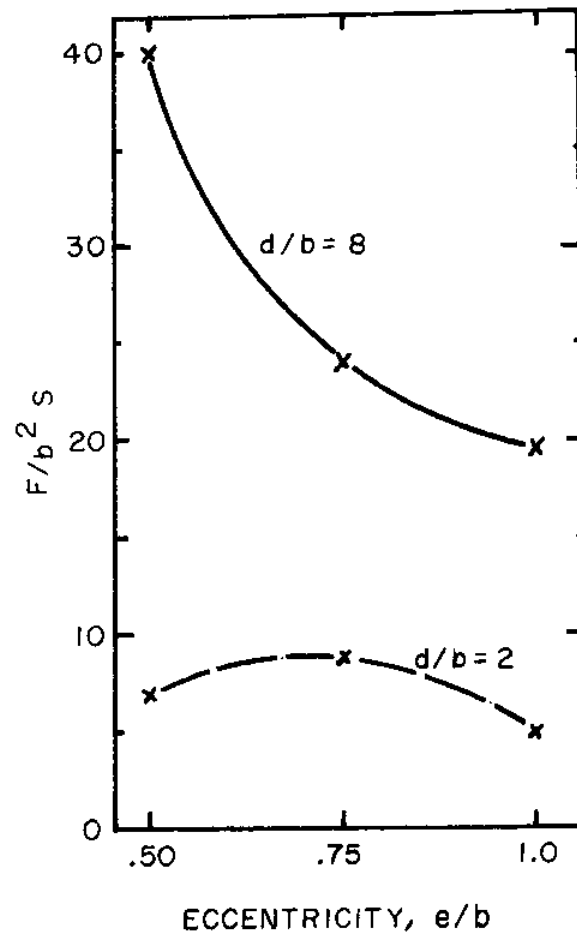


FIGURE 20 DIMENSIONLESS PULLOUT FORCE TERM VS DIMENSIONLESS PULLOUT CABLE ECCENTRICITY FOR DRY SAND

Continuing this method of analysis to the marine sediment results, Figure 21 reports the dimensionless relation between F/b^2S and α for values of d/b in this material. Kananyan did not perform any tests into a saturated cohesive soil and no other inclined pullout tests could be found, so Figure 21 shows values only for $d/b = 2$ and 8 .

Figure 22 shows the plot of the dimensionless pullout force term against e/b for the two values of d/b examined in this study. No other data were available for comparison.

Dimensionless design relationship. Recognizing that it would be valuable if a valid relationship between all four of the dimensionless variables that had been developed could be displayed, it was decided to multiply the three π -terms, F/b^2S , α , and e/b together and plot the result against d/b . Since the resulting multiple term would contain the factor b to some power and would be plotted against the same factor in the other term, it was necessary to determine that this combination of factors would not represent a spurious correlation as described by Benson (5) and by Yalin and Kamphuis (53). Examination of Figures 19 and 21, which show the relationship of the dimensionless

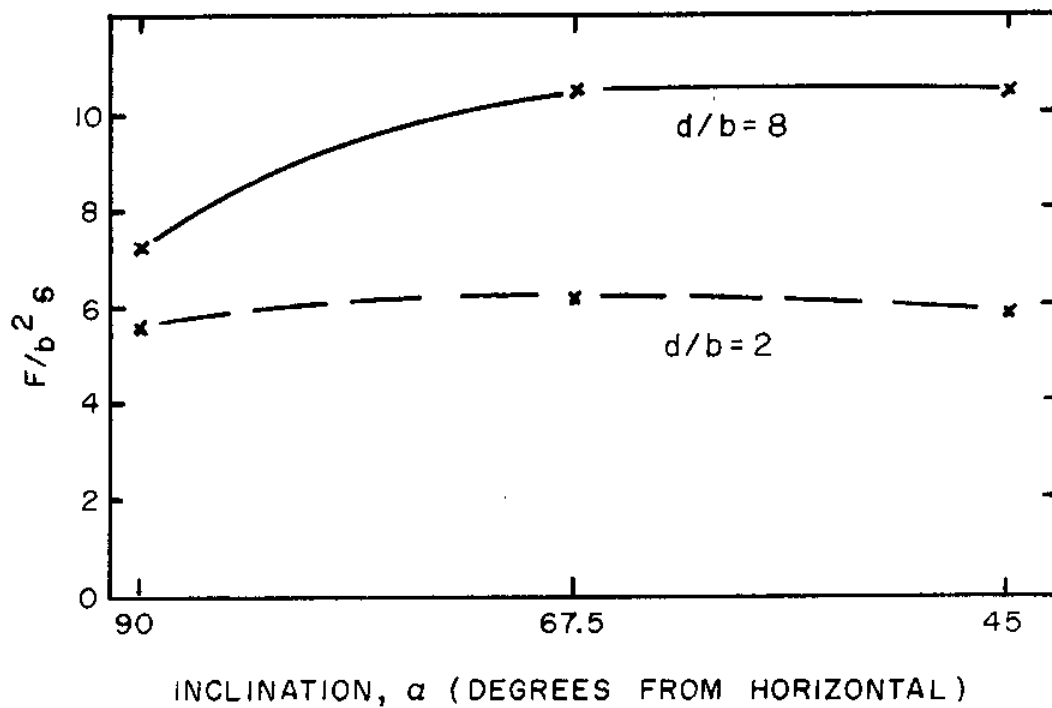


FIGURE 21 DIMENSIONLESS PULLOUT FORCE TERM VS
DIMENSIONLESS PULLOUT CABLE INCLINATION FOR
MARINE SEDIMENT

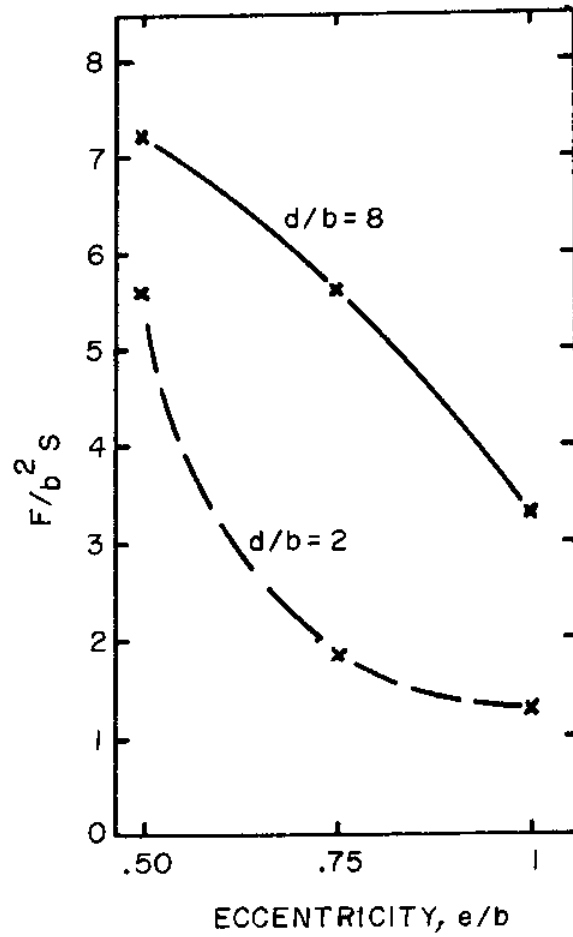


FIGURE 22 DIMENSIONLESS PULLOUT FORCE vs
DIMENSIONLESS PULLOUT CABLE ECCENTRICITY
FOR MARINE SEDIMENTS

inclination term, revealed that for both materials studied these factors had an almost direct linear relation. This would indicate that the α term should be in the numerator of the combined force term. Studying Figures 20 and 22, which show the force term relative to the eccentricity term, indicated that the relationship was inverse but not direct. In order to prove the validity of using a product of these two dimensionless terms, it was necessary to examine the relationship between the force term and the inverse of the eccentricity term. This plot is shown in Figure 23 for both dry sand and marine sediments. For dry sand, it can be seen that the inverse eccentricity term b/e plots quite well through the origin indicating a valid relationship. For marine sediments, the validity of the relationship is evident for the case where $d/b = 8$ and could be considered to exist with some validity for the $d/b = 2$ case. Accordingly, it was felt that if a relationship between the multiple of three of the π -terms and the remaining one could be shown, it would be valid and not spurious even though it would contain common dimensional parameters along both axes. This result is in accordance with the statement made by Yalin and Kamphuis (53) on page 263 of their article as follows:

The usual case of spurious correlation is the appearance of common quantities along both co-ordinate axes. This is true for both a dimensional and dimensionless system. This must not be confused with the appearance of common dimensional parameters along both co-ordinate axes when dimensionless variables are plotted against each other.

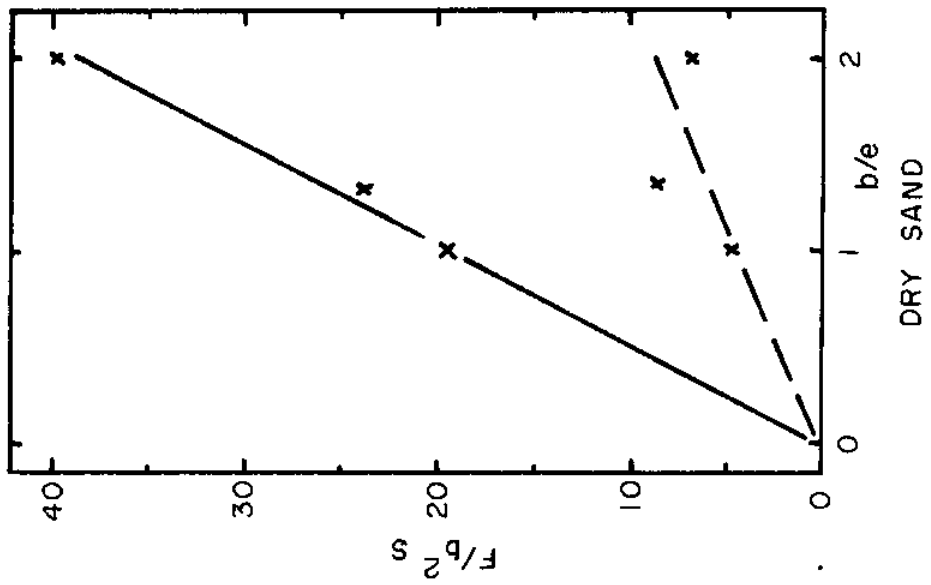
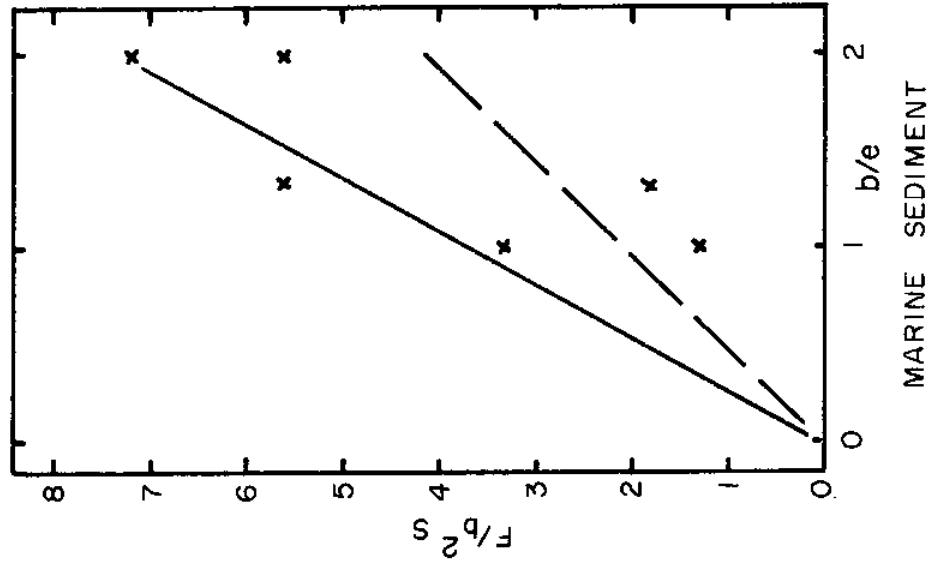


FIGURE 23 DIMENSIONLESS PULLOUT FORCE TERM vs DIMENSIONLESS INVERSE ECCENTRICITY TERM FOR DRY SAND AND MARINE SEDIMENT

The resulting multiple π -term was determined to be $F \propto e/b^3 S$. Figure 24 shows the observed data reduced to this multiple term as a function of d/b . As can be seen, the data when presented in this manner fall into two distinct groupings: one for tests run in the dry sand material; the other for tests in the marine sediments. This division of data seems reasonable since the two distinct types of materials - granular and cohesive - would be expected to fail in different manners according to the usual understanding of soil mechanics.

The observed data for the dry sand and marine sediment soils from this study were programmed through the Texas A&M University IBM 360/65 computer using the Wilson-Goodlet Multiple Regression Program prepared by the Institute of Statistics, Texas A&M University. This is a flexible, general purpose multiple linear (least squares) regression program, written in Fortran IV.

For the sand data, the results obtained were:

$$\text{Function: } \frac{F}{b^3} \frac{e}{S} = -0.6 + 3.8 \frac{d}{b} \quad (13)$$

Data Correlation Factor: $R = 0.98$

These results indicate very good correlation of the data to the calculated straight line function. This calculated line has been plotted in Figure 24. The dashed lines shown on each side of the solid calculated line indicate the envelope of the data points observed in this study. As can be seen in Figure 24, this

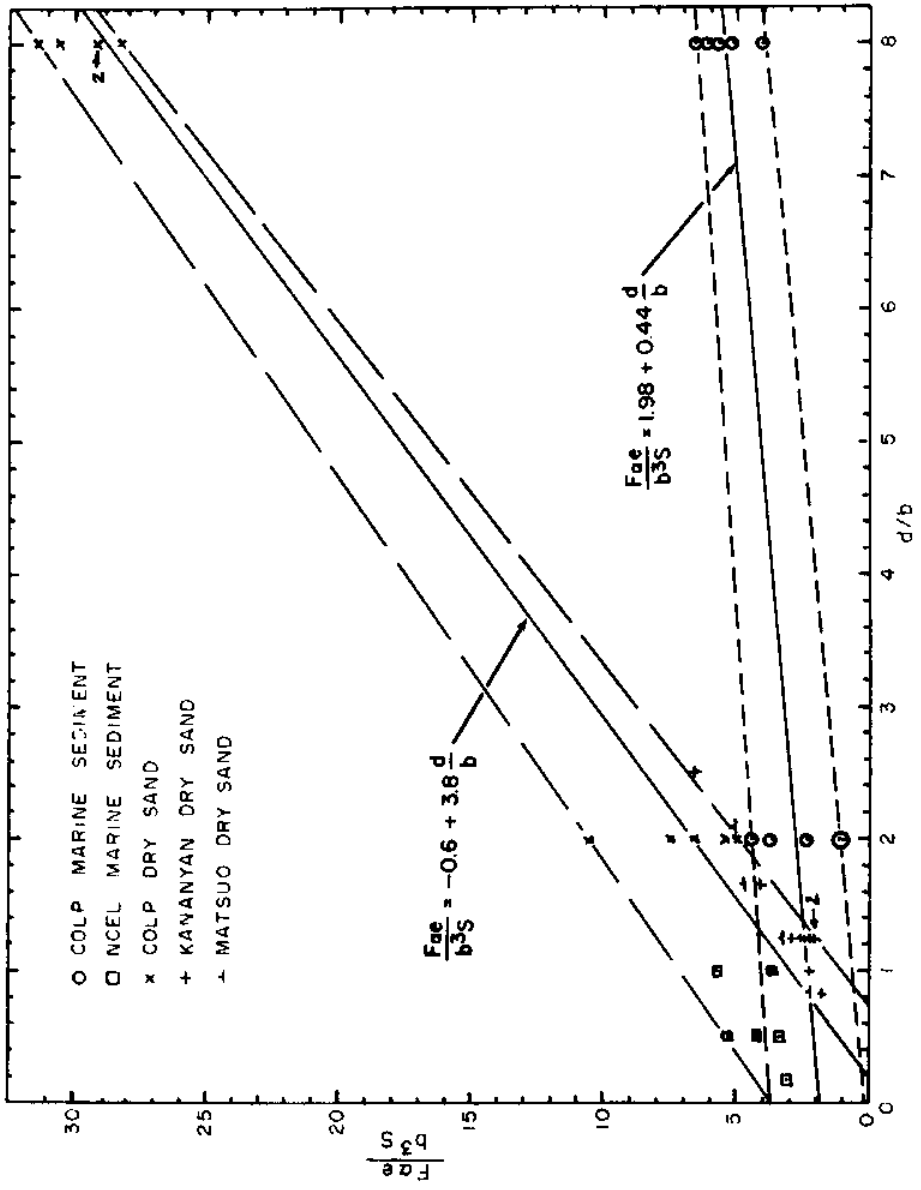


FIGURE 24 DIMENSIONLESS PULLOUT FORCE TERM vs DIMENSIONLESS BURIAL DEPTH FOR DRY SANDS AND MARINE SEDIMENTS

envelope encompasses all of the data points from Kananyan's (22) and Matsuo's (31) studies in sand with two exceptions, both of which are just outside the lower dashed line.

For the marine sediment pullout data, the results obtained from the computer calculation were:

$$\text{Function: } \frac{F}{b^3} \frac{\alpha e}{S} = 1.98 + 0.44 d/b \quad (14)$$

$$\text{Data Correlation Factor : } R = 0.82$$

These results indicate reasonably good correlation of the data to the calculated straight line function. The calculated straight line has been plotted in Figure 24. The dotted lines shown on each side of the calculated line indicate the limits of the observed data points for this material. With three exceptions, selected data from the Naval Civil Engineering Laboratory as reported by Lee (27) fall within this envelope.

The two equations listed above could be used to obtain a value for an estimated maximum pullout force required to withdraw an object that is embedded in dry sand or in marine sediments when subjected to an inclined or eccentric load application.

CONCLUSIONS

Two-dimensional Investigation

On the basis of the results obtained from the two-dimensional experiments conducted in this study, the following conclusions seen to be warranted:

1. Use of the two-dimensional roller bearing experimental technique to observe particle motions during anchor pullout in dense, granular, cohesionless materials appears to be justified based on the similarity of maximum pullout forces recorded when compared to those in a three-dimensional model anchor pullout test in dry, dense Ottawa sand.
2. The differences in particle displacements, failure lines, open void locations, and particle counterflow for inclined and eccentric pullout load applications in a dense, granular, cohesionless material can be seen from the photographs taken during these experiments. The primary failure mode appears to be general shear in all of the shallow-buried tests and local shear in all of the deeply buried tests.
3. The total number of particles being displaced increases in all cases as the load application inclination angle approaches 45°; but decreases as the point of load application moves from the center of the anchor plate to one end.

Three-dimensional Investigation

On the basis of the results from the three-dimensional experiments conducted, the following conclusions seem to be warranted:

1. The maximum force required during pullout of a model plate anchor increases as the load

application angle changes from vertical to 45° for the three soil materials tested in the shallow-burial case and for dense, dry sand and marine sediment in the deeply-buried case. However, the rate of increase in maximum pullout force as the inclination angle changes from vertical to 45° is much smaller in marine sediments than in dense, dry sand at both burial depths. (Apparently the influence of pore water pressures in the submerged, dense sand causes an anomalous behavior in the deeply-buried inclined and eccentric pullout cases. To better understand the cause of this behavior, future experiments in which pore pressures can be measured are recommended.)

2. The maximum force required during pullout of a model plate anchor decreases as the point of load attachment is moved from the center to one edge of the plate for the three materials tested in the shallow-burial case and for dense, dry sand and marine sediments in the deeply-buried case. The rate of decrease in the maximum pullout force required as the load application point is moved to one edge is similar for all materials in the shallow-burial case, but is much less than that of the dry sand in the deeply-buried case.
3. A dimensionless relationship between the maximum pullout force, angle of inclination, eccentricity of load application and soil shear strength as a function of burial depth was developed by dimensional analysis methods and appears to be valid. The experimental data from this study presented in these dimensionless parameters fall into two distinct groupings, one for dry sand and the other for marine sediment. Available data from other investigators in both materials, falls, with few exceptions, within the limits of the observed data from this study. A Wilson-Goodlet Multiple Regression Analysis of the dimensionless data described above gives two equations which could be used to obtain a value for an estimated maximum pullout force required to withdraw an object embedded in dry

sand or marine sediment when subjected to
an inclined or eccentric load application.

RECOMMENDATIONS

The following recommendations for future research in the area covered by this study are made:

1. An investigation using the two-dimensional roller bearing experimental technique of the effect of depth of burial on the failure mode (general or local) experienced during pullout. Tests at $d/b = 3, 4, 5, 6,$ and 7 are recommended. The addition of some viscous fluid to the roller bearing array could be used to allow investigation of particle displacements during anchor withdrawal from cohesive materials.
2. An investigation of inclined and eccentric withdrawal of anchors from submerged dense sand with equipment to measure changes in pore pressures at various locations during displacement to reach a better understanding of the behavior noticed in these cases during this study.
3. Additional inclined and eccentric three-dimensional pullout tests in dry sand and marine sediment at values of $d/b = 4, 6, 10$ and 12 to improve the validity of the dimensionless equation obtained in this study.

BIBLIOGRAPHY

1. Baker, W. L. & R. L. Kondner, "Pullout Load Capacity of a Circular Earth Anchor Buried in Sand", *Highway Research Record #108*, Highway Research Board, NAS, Washington, D.C., 1966, p. 1-10.
2. Balla, A., "Resistance to Breaking-Out of Mushroom Foundations for Pylons", *Proceedings*, Fifth International Conference on Soil Mechanics and Foundation Engineering, Paris, 1961, V. 1, p. 569-76.
3. Banchemo, Louis A., "Long Term, Deep Ocean Mooring of Current Measuring Arrays", *Preprint OTC 1294*, Second Annual Offshore Technology Conference, Houston, Texas, April 22-24, 1970, p. II-645-II-654.
4. Bembem, S. M., M. Kupferman, and E. H. Kalajian, "The Vertical Holding Capacity of Marine Anchors in Sand and Clay Subjected to Static and Cyclic Loadings", *Final Report to Naval Civil Engineering Laboratory Under Contract N 62399-70-C-0025*, University of Massachusetts, Amherst, Massachusetts, 1972.
5. Benson, M. A. "Spurious Correlation in Hydraulics and Hydrology", *Journal*, Hydraulics Division, ASCE, July 1965, p. 35-41.
6. Bryant, W. R., L. J. Thompson, and S. H. Carpenter, "Properties of Marine Sediments as Related to Penetration", *Rapid Penetration of Terrestrial Materials*, J. L. Colp, Editor, Texas Engineering Experiment Station, College Station, Texas, 1972.
7. Buckingham, E., "On Physically Similar Systems", *Physics Review*, Vol. 4, p. 354-376, 1914.
8. Colp, J. L., "An Experimental Investigation of the Continuous Penetration of a Blunt Body into a Simulated Cohesionless Soil", *M.S. Thesis*, University of New Mexico, Albuquerque, N.M., 1965.
9. Colp, J. L., "Terradynamics: A Study of Projectile Penetration of Natural Earth Materials", *Report SC-DR-68-275*, Sandia Laboratories, Albuquerque, New Mexico, June 1968, 61 p, p. 10-11.

10. Dantz, P. A., "The Padlock Anchor - A Fixed Point Anchor System", *Technical Report R577*, U. S. Naval Civil Engineering Laboratory, Port Hueneme, California, May 1968.
11. Daubin, Scott C., "Mooring Design & Performance of Oceanographic Buoys", *Buoy Technology*, Transactions, 1964 Buoy Technology Symposium, Washington, D.C., March 24-25, 1964, p. 91-105.
12. DeHart, R. C. & C. T. Ursell, "Force Required to Extract Objects from the Deep Ocean Bottom", *Report*, Southwest Research Institute, San Antonio, Texas, Sept. 1967, 9 p.
13. Dove, H.L., "Investigations on Model Anchors", *Transactions*, Institution of Naval Architects, v. 92, n. 4, Oct. 1950, p. 351-75.
14. Dove, H. L. & G. S. Ferris, "Development of Anchors", *Transactions*, Royal Institution of Naval Architects, v. 102, n. 4, October 1960, p. 535-54.
15. Esquivel-Diaz, R. F., "Pullout Resistance of Deeply Buried Anchors in Sand", *Soil Mechanics Series No. 8*, Duke University, Durham, N.C., 1967, 57 p.
16. Farlow, John S., "A Great Lakes Unmanned Weather Buoy and Current Measuring System", *Buoy Technology*, Transactions, 1964 Buoy Technology Symposium, Washington, D. C., March 24-25, 1964, p. 619-28.
17. Farrell, K. P., "Improvements in Mooring Anchors", *Transactions*, Institution of Naval Architects, v. 92, n. 4, Oct. 1950, p. 335-50.
18. Frost, Honor, *Under the Mediterranean--Marine Antiquities*, Prentice-Hall, Englewood Cliffs, N.J., 1963, 278 p.
19. Gerard, Robert D., "Taut-Line Navigation Buoys Used in Thresher Search", *Buoy Technology*, Transactions 1964, Buoy Technology Symposium, Washington, D.C., March 24-25, 1964, p. 197-203.
20. Howard, W. E. & R. K. James, "Investigation of Anchor Characteristics by Means of Models", Massachusetts Institute of Technology, 1933.

21. Kalajian, E. H. & S. M. Bemben, "The Vertical Pullout Capacity of Marine Anchors in Sand" *THEMIS Report No. THEMIS-UM-69-5*, AD 689 522.
22. Kananyan, A. S. "Experimental Investigation of the Stability of Bases of Anchor Foundations", *Osnovaniya, Fundamenty i Mekhanika Gruntov* (Soil Mechanics & Foundations), v. 4, n. 6, Nov-Dec 1966, p. 387-92.
23. Keays, K., "Static Mooring--A Review of the State of the Art", *Naval Engineers Journal*, August 1970, p. 63-70.
24. Lambe, T. W. & R. V. Whitman, *Soil Mechanics*, John Wiley & Sons, Inc., New York, 1969.
25. Land, E. S., "Development in Ground Tackle for Naval Ships", *Transactions*, Society of Naval Architects and Marine Engineers, v. 42, 1934, p. 164-74.
26. Leahy, William H. & J. M. Farrin, Jr., "Determining Anchor Holding Power from Model Tests", *Transactions*, Society of Naval Architects & Marine Engineers, V. 43, 1935, p. 105-20.
27. Lee, H. J., "Unaided Breakout of Partially Embedded Objects from Cohesive Seafloor Soils", *Technical Report R 755*, U. S. Naval Civil Engineering Laboratory, Port Hueneme, California 93043, February 1972.
28. Liu, C. L., "Ocean Sediment Holding Strength Against Breakout of Embedded Objects", *Technical Report*, U. S. Naval Civil Engineering Laboratory, Port Hueneme, California, 1969.
29. Lucking, D. F., "The Experimental Development of Anchors for Seaplanes", *Transactions*, Institution of Naval Architects, 1936, p. 201-23.
30. Mariupolskii, L. G., "The Bearing Capacity of Anchor Foundations," *Osnovaniya, Fundamenty i Mekhanika Gruntov* (Soil Mechanics and Foundation Engineering), v. 3, n. 1, Jan-Feb, 1965, p. 26-32.
31. Matsuo, M., "Study of Uplift Resistance of Footings", *Soils and Foundations* (Japan), v. 7, n. 1, Dec. 1967, p. 1-37.
32. Matsuo, M. "Study of Uplift Resistance of Footings", *Soils and Foundations* (Japan), v. 8, n. 1, Mar. 1968, p. 18-48.

33. Meyerhof, G. G. and J. I. Adams, "The Ultimate Uplift Capacity of Foundations", *Canadian Geotechnical Journal*, v. 5, n. 4, Nov. 1968, p. 225-44.
34. Muga, B. J., "Breakout Forces", *Technical Note N-863*, U. S. Naval Civil Engineering Laboratory, Port Huenema, California, Sept 1966, 24 p.
35. Muga, Bruce J. "Bottom Breakout Forces", *Proceedings*, Conference on Civil Engineering in the Oceans, San Francisco, Sept 1967, p. 569-600.
36. Muga, Bruce J., "Ocean Bottom Breakout Forces", *Technical Report R-591*, U. S. Naval Civil Engineering Laboratory, Port Hueneme, California, June 1968, 140 p.
37. Murff, J. D. & H. M. Coyle, "Projectile Penetration into Earth Media", *Technical Report Project 678*, Texas A&M Research Foundation, College Station, Texas, July 1970, 127 p, p. 4.
38. Murff, J. D. & H. M. Coyle, "Projectile Penetration into Earth Media", *Technical Report Project 734*, Texas A&M Research Foundation, College Station, Texas, June 1971, 219 p., p. 3,4.
39. Nowlin, W. D., Jr., "Selected Environmental Parameters at Buoy Mooring Sites in the Gulf of Mexico", *Report*, Electro Dynamic Division of General Dynamics, San Diego, California, August 13, 1971.
40. Robinson, K. E. and H. Taylor, "Selection and Performance of Anchors for Guyed Transmission Towers", *Canadian Geotechnical Journal*, v. 6, 1969, p. 119-37.
41. Smith J. Eugene, "Investigation of Embedment Anchors for Deep Ocean Use", *Paper #66-PET-32*, American Society of Mechanical Engineers, 1966.
42. Smith, J. Eugene, "Investigation of Embedment Anchors for Deep Ocean Use", *Technical Note N-834*, U. S. Naval Civil Engineering Laboratory, Port Hueneme, California, July 1966.

43. Smith, J. Eugene, "Explosive Anchor for Salvage Operation-- Progress and Status", *Preprint OTC 1504*, Third Annual Offshore Technology Conference, Houston, Texas, April 19-21, 1971, p. II-859-II-872.
44. Sutherland, H. B., "Model Studies for Shaft Raising Through Cohesionless Soils," *Proceedings*, Sixth International Conference on Soil Mechanics & Foundation Engineering, Montreal, 1965, v. 2, p. 410-3.
45. Thompson, L. J., "Summation of the Work of the Terramechanics Laboratory 1968-1969", *Technical Report Project 596-1*, Texas A&M Research Foundation, College Station, Texas, August 1969, 30 p., p. 20.
46. Thompson, L. J., "Projectile Penetration Theory", *Rapid Penetration of Terrestrial Materials*, J. L. Colp, Editor, Texas Engineering Experiment Station, College Station, Texas, 1972.
47. Thorpe, T. & K. P. Farrell, "Permanent Moorings", *Transactions*, Institution of Naval Architects, v. 90, 1948, p. 111-53.
48. Tolson, B. E., "A Study of the Vertical Withdrawal Resistance of Projectile Anchors", *M. S. Thesis*, Texas A&M University, College Station, Texas, May 1970, 46 p.
49. Towne, R. C., "Mooring Anchors", *Transactions*, Society of Naval Architects & Marine Engineers, v. 67, 1959, p. 290-307.
50. Tudor, Walter J., "Mooring and Anchoring of Deep Ocean Platforms", *Proceedings*, Conference on Civil Engineering in the Oceans, San Francisco, Sept. 1967, p. 351-90.
51. Vesic, A. S., "Cratering by Explosives as an Earth Pressure Problem", *Proceedings*, Sixth International Conference on Soil Mechanics and Foundation Engineering, Montreal, 1965, v. 2, p. 427-32.
52. Vesic, A. S., "Breakout Resistance of Objects Embedded in Ocean Bottom", *Journal*, Soil Mechanics & Foundations Division, ASCE, Sept. 1971, p. 1183-1205.
53. Yalin, M. S. and J. W. Kamphuis, "Theory of Dimensions and Spurious Correlation", *Journal of Hydraulic Research*, International Association for Hydraulic Research, v. 9, n. 2, 1971, p. 249-265.

APPENDIX

 DIMENSIONAL ANALYSIS

Dimensional analysis, described by Buckingham (7) in his π -theorem is a standard method used by many researchers to determine the functional relationships between the primary physical constants involved in physical phenomena. This analysis is often useful in providing a simple basis for the possible correlation of the results obtained from small-scale model tests.

The π -theorem says that a physical phenomenon which is a function of n physical quantities involving m fundamental units of dimensions can be described in the following functional form:

$$f(\pi_1, \pi_2, \dots, \pi_{n-m}) = 0 \quad (A-1)$$

where the π -terms are the $(n-m)$ dimensionless products of the n physical properties.

The primary physical quantities considered in this anchor pullout study are listed below together with their fundamental units:

Maximum Pullout Force	F	M
Angle of Inclination	α	L/L
Eccentricity	e	L
Burial Depth	d	L
Anchor Plate Diameter	b	L
Soil Shear Strength	S	M/L ²

Expressing these primary physical quantities in the functional form, gives:

$$F = f(\alpha, e, d, b, S) \quad (\text{A-2})$$

The fundamental dimensions in which these primary physical properties are expressed are M and L.

Therefore, the number of dimensionless π -terms to be found correspond to $(n-m)$ which turns out to be equal to $6-2$ or 4 .

By selecting the quantity b as a repeating variable, inspection of Equation A-2 reveals the following dimensionless terms:

$$\pi_1 = \alpha, \quad \pi_2 = d/b, \quad \pi_3 = e/b.$$

This then leaves Equation A-2 in the form of:

$$F = f(b, S) \quad (\text{A-3})$$

Using the methods of the π -theorem, the following transformations are made:

$$[F]^{n_1} = [b]^{n_2} [S]^{n_3} \quad (\text{A-4})$$

Substituting the fundamental units for each primary physical property gives:

$$[M]^{n_1} = [L]^{n_2} [ML^{-2}]^{n_3} \quad (\text{A-5})$$

Continuing the analytical method gives two equations in three unknowns as follows:

$$M: \quad n_1 = n_3 \quad (A-6)$$

$$L: \quad 0 = n_2 - 2n_3 \quad (A-7)$$

Solving these equations for n_2 and n_3 in terms of n_1 gives:

$$n_3 = n_1 \quad (A-8)$$

$$n_2 = 2n_3 = 2n_1 \quad (A-9)$$

These values can be substituted back into Equation A-4 to get:

$$[F]^{n_1} = [b]^{2n_1} [S]^{n_1} \quad (A-10)$$

Rearranging Equation A-10 gives:

$$[F]^{n_1} [b]^{-2n_1} [S]^{-n_1} = [0] \quad (A-11)$$

Collecting exponents results in:

$$\left[\frac{F}{b^2 S} \right] = [0] \quad (A-12)$$

Equation A-12 shows the fourth dimensionless π -term obtained from this analysis.

